Reliability Engineering and System Safety 261 (2025) 111118

Contents lists available at ScienceDirect

Reliability Engineering and System Safety

journal homepage: www.elsevier.com/locate/ress

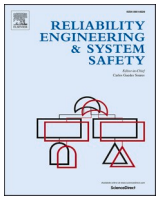

Enabling autonomous navigation: adaptive multi-source risk quantification in maritime transportation

Lichao Yang [a,b,d], Jingxian Liu [a,b,e], Qin Zhou [d,*], Zhao Liu [a,b,*], Yang Chen [a,b], Yukuan Wang [a,b,e], Yang Liu [b,c]

[a] School of Navigation, Wuhan University of Technology, Wuhan, 430063, China
[b] State Key Laboratory of Maritime Technology and Safety, Wuhan University of Technology, Wuhan, 430063, China
[c] Intelligent Transportation System Research Center, Wuhan University of Technology, Wuhan, 430063, China
[d] Centre for Risk Research, Department of Decision Analytics and Risk, Southampton Business School, University of Southampton, UK
[e] Sanya Science and Education Innovation Park, Wuhan University of Technology, Hainan Sanya, 572024, China

ARTICLE INFO

Keywords:
Intelligent transportation systems
AIS data
Heterogeneous navigation risks
Spatiotemporal risk modelling
Adaptive risk fusion

ABSTRACT

Current studies on maritime navigation risks often overlook interactions between ships, dynamic surroundings, and static environmental factors, limiting insights into navigation safety in complex scenarios. This research presents an innovative methodology to quantify and integrate multi-source heterogeneous navigation risks, enabling a comprehensive assessment of overall risk levels. The framework comprises four components. First, a spatiotemporal risk monitoring domain model, developed using historical AIS data, incorporates risk monitoring and forbidden domains, enabling precise localisation and timing of risk evaluation. Second, heterogeneous navigation risk evaluation functions, addressing dynamic target and static environment risks, capture ships' varying sensitivities to diverse risk sources. Third, risk quantification methods evaluate dynamic risks from temporal and spatial perspectives while categorising static risks into three types. Finally, an adaptive fusion method hierarchically aggregates multi-source risk data into a unified profile, reflecting navigators' risk perception. Real-world AIS data validate the framework, constructing spatiotemporal risk models for three ship types and analysing navigation scenarios such as crossing, overtaking, and multi-ship encounters. Results demonstrate the framework's capability to enhance precision in navigation risk assessment, providing actionable insights and robust support for autonomous navigation and intelligent maritime systems. This methodology offers a promising tool for advancing safety in complex maritime environments.

1. Introduction

Maritime transport is responsible for over 90 % of global trade volume and serves as a cornerstone of the global economy [1,2]. Ensuring the safety of ships, which constitute the backbone of the maritime transport industry, is crucial for its sustainable development [3,4]. The integration of big data analytics, Artificial Intelligence (AI) and smart navigation systems is driving a transformative shift toward ship automation. Autonomous navigation systems are emerging as a fundamental component of maritime intelligence [5–7]. Accurate risk assessment in maritime navigation is paramount for enabling these autonomous systems, supporting both optimal route planning and effective collision avoidance strategies.

Current research on ship navigation risk assessment primarily follows three avenues. The first focuses on collision risk, where existing methodologies can be broadly divided into index-based and safety boundary approaches [8–10]. Index-based methods are widely adopted for their simplicity and computational efficiency [8]. However, these approaches often suffer from oversimplified assumptions. For instance, they frequently overlook crucial variables such as ship size distributions. Moreover, they tend to rely heavily on subjective expert judgements, which may introduce bias into the analysis. Safety boundary methods, subdivided into collision diameter and ship domain models, attempt to address these limitations by refining risk perimeters [9]. Ship domain models can be categorised into three distinct types: empirical [11], knowledge-based [12] and analytical approaches [13–15]. Each type presents unique challenges in maritime applications [13]. Empirical models, whilst data-driven, are constrained by their heavy reliance on

* Corresponding authors.
E-mail addresses: q.zhou@soton.ac.uk (Q. Zhou), zhaoliu@whut.edu.cn (Z. Liu).

https://doi.org/10.1016/j.ress.2025.111118
Received 19 December 2024; Received in revised form 11 March 2025; Accepted 7 April 2025
Available online 8 April 2025

historical datasets. Knowledge-based models incorporate expert experience but may introduce subjective biases into the assessment process. Analytical models, despite their mathematical rigour, often prove too specific to particular scenarios, which not only limits their broader application but also increases their computational demands.

A second research direction addresses grounding and allision risks. The assessment of grounding risks predominantly follows two methodological approaches: probability-based analysis [16] and consequence-based evaluation [17]. In contrast, allision risk assessment is more object-specific, requiring distinct analytical frameworks for different marine structures. These structures encompass fixed installations such as bridges [18] and offshore wind turbines [19], as well as maritime infrastructure, including production platforms [20] and navigational aids [21]. Despite their contributions, these studies often suffer from oversimplified models and limited generalisability across diverse navigational scenarios.

The third research direction investigates the complex interplay of navigational risks and their underlying causes. Various analytical approaches have been developed to understand these interactions. These include probabilistic methods such as Bayesian networks [22] and N-K models [23], human-centric frameworks like Human Factors Analysis and Classification System (HFACS) [24], and dynamic modelling approaches, including system dynamics [25] and ship domain safety methods [11]. These techniques have proved particularly valuable in analysing complex scenarios, such as multi-ship encounters in congested waterways. Whilst these methodologies have advanced our understanding of specific risk scenarios, they fall short in providing a holistic assessment of heterogeneous navigational risks. Ships routinely encounter multiple risk sources simultaneously—including collision, grounding and allision risks—within dynamic maritime environments. These risks often manifest in complex combinations, creating intricate risk landscapes that existing models struggle to capture fully. The development of a robust framework for evaluating such multi-source heterogeneous risks is crucial, particularly as risk assessment underpins critical functions in autonomous navigation, including route planning and collision avoidance systems.

In general, most current research on maritime navigation risk assessment focuses on the risk of ship collisions. Li et al. [26] designed a data-driven collision risk analysis model to investigate the impact of COVID-19 on global ship collision risk. Xin et al. [27] developed a traffic clustering approach to identify high-risk multi-ship collision areas in complex waterways. These studies on the collision risk in large-scale waterways provide reference for port management decision-making, but have limited guidance for ship route planning and collision avoidance decision-making. Therefore, some studies have shifted to the perspective of individual ships in explaining collision risk. Liu et al. [28] were the first to introduce the elliptical ship domain into the velocity obstacle method and assessed ship collision risk from the perspective of risk evolution. Other studies have focused on specific types of risks, such as grounding [29,30], allision [18], static risks related to Port State Control (PSC) inspections [31], and pirate threats [1,32], providing decision support for addressing individual risks. However, these studies mostly focus on a single type of risk, lacking a comprehensive assessment of the heterogeneous risks from multiple sources during ship navigation. Therefore, it is necessary to design a tool from the perspective of ship officers to accurately reflect the comprehensive risk level of the heterogeneous risks from multiple sources during ship navigation.

Based on the identified challenges, this paper presents several key contributions.

1) It develops an advanced risk monitoring model that effectively integrates historical Automatic Identification System (AIS) data mining with real-time risk assessment. Unlike existing approaches that rely on simplified assumptions, this model captures and replicates the complex cognitive patterns and timing of risk assessments conducted by experienced ship officers. This innovation enhances the precision of maritime risk predictions by closely aligning with actual navigator decision-making processes.
2) It introduces sophisticated heterogeneous risk evaluation functions that systematically differentiate and quantify dynamic and static risks within a unified framework. In contrast to traditional methods that treat all risks uniformly, these functions account for officers' varying sensitivities to different types and directional hazards. This advancement enables a more nuanced and realistic understanding of navigational risks in complex maritime environments.
3) An adaptive risk quantification method is proposed that surpasses conventional approaches by comprehensively integrating both spatial and temporal dimensions. This method presents an effective approach to assessing the overlap between spatio-temporal monitoring domains. Unlike traditional methods that focus on either spatial or temporal aspects, this integrated approach significantly improves both early warning capabilities and risk assessment accuracy.
4) The research sets up a comprehensive multi-source risk fusion model that effectively integrates diverse navigation risks. This model prevents risk overaccumulation while maintaining sensitivity to individual risk sources.

Together, these contributions provide a robust framework for enhancing the understanding and management of navigational risks in complex maritime environments, thereby fostering safer maritime operations and informed decision-making.

The remainder of the paper is organised as follows: Section 2 presents the literature review, summarising the main research directions in ship navigation risk assessment. Section 3 introduces our methodological framework in detail. This encompasses four main components: the spatiotemporal risk monitoring domain model, heterogeneous navigation risk evaluation functions, a novel approach for quantifying multi-source heterogeneous risks, and an adaptive fusion method for integrating these risks. Section 4 provides the experimental analysis of the framework, while Section 5 discusses the findings and their implications. Finally, conclusions are highlighted in Section 6.

2. Literature review

Ship navigation risk research employs a ship-centric approach to examine interaction-induced hazards in maritime operations. This field encompasses three fundamental risk categories: ship-to-ship collisions, grounding incidents in shallow waters, and structural damages resulting from the complex interactions between ships and their operational environment. Based on the nature of risk sources, this study categorises ship navigation risks into two broad classifications: dynamic target risks, which involve mobile entities in the maritime environment, and static environmental risks, which pertain to fixed geographical and infrastructural elements.

2.1. Dynamic target risk assessment

Dynamic target risk refers to the risk generated from interactions between a ship and other target ships during navigation, namely the risk of collisions between ships. Based on the analysis of numerous maritime traffic accidents, ship collisions constitute a significant portion of all accident types and are a key focus of maritime traffic risk research [33]. The evaluation of ship navigation risks serves as a vital foundation for navigational route design and collision avoidance manoeuvres for officers, as well as being a critical component in achieving autonomous ship navigation. The microscopic approach to ship collision risk assessment originates from the ship officer's perspective, focusing on sensing the collision risk in the ship's surrounding environment and making collision avoidance decisions accordingly. This method can be subdivided into the index method and the safety boundary method [8,9].

The index method involves using geometric parameters as indicators to assess encounter situations or combining them into new formulas to evaluate potential ship collision risks [8]. Owing to its simplicity and ease of use, this method has become the most frequently applied approach in collision avoidance decision-making for ship officers. Research in this area has been conducted along three lines: examining officers' sensitivity to different parameters, improving the model's perception of ship encounter scenarios, and designing risk quantification formulas tailored to specific situations. 1) Exploring the contribution of different indicators to collision risk and using expert knowledge [34], fuzzy mathematics [35], and neural networks [36] to determine indicator weights. 2) Introducing additional parameters like mutual distance, relative bearing, and relative speed, with the aim of more fully reproducing ship encounter scenarios [37,38]. 3) Developing risk quantification formulas for situations such as multi-ship encounters [39] and ship-bridge collisions [40]. While the index method offers simplicity in modelling and relatively fast computation, it still faces several challenges. For instance, the index method often relies on overly idealised conditions, which do not reflect the real movement of ships. It abstracts ships and obstacles as point masses, overlooking the impact of object size on collisions and assuming all targets continue their current motion states unchanged. Indicator selection and weight determination often lack data or theoretical backing, and their accuracy depends heavily on the subjective influence of the selected experts.

The safety boundary method quantifies ship collision risks by using the spatiotemporal proximity between ships to measure their closeness [9]. Relevant research first introduced the concept of collision diameter to describe the spatiotemporal relationships between ships, and the subsequent expansion of this concept contributed to the creation of ship domains [41,42]. Researchers have investigated historical data, prior knowledge, and specific scenario analyses, developing three types of ship domain models: empirical ship domain models [11], knowledge-based ship domain models [12], and analytical ship domain models [13–15]. Each of these modelling methods has unique features, and they are not contradictory, allowing flexible combinations [13]. The safety boundary method partially addresses the limitations of the index method and, due to its modelling flexibility, has seen broad application. However, it still has several challenges. For example, the collision diameter method sets a threshold for relative distance between ships or between ships and obstacles but does not factor in the ships' dynamic states. It classifies encounters exceeding this threshold as safe, neglecting the ambiguity of collision risks. The suitability of empirical ship domain models is highly dependent on the quality and volume of data, and handling massive datasets raises the computational cost of this method. The accuracy of knowledge-based ship domain models heavily relies on proper extraction of prior knowledge features and can also be influenced by experts' subjective judgment. Analytical ship domain models are typically designed for specific environments, leading to limited generalisability. Moreover, they involve more parameters and are more complex than other models.

2.2. Static environmental risk assessment

Static environmental risk refers to the risks arising from interactions between a ship and relatively fixed environmental factors during its navigation [43]. For instance, risks such as grounding or damage can occur when a ship enters non-navigable areas, such as shallow waters, lands, reefs, or buoys. At present, research on the evaluation of grounding and damage risks is much less extensive compared to ship collision risks.

Regarding grounding, the Pederson [44] models estimate the risk of ship grounding by integrating the probability density function of traffic flow at the interface between the ship's navigation and obstacles. Likewise, Youssef et al. [45] analysed the statistical characteristics of random variables related to ship grounding accident data in order to estimate the probability of ship grounding. Khaled et al. [46] analysed the maritime accident records in Bangladesh from 1981 to 2013 using the IWRAP MK2 software. Besides statistical analysis, fault tree and Bayesian network are also frequently used to evaluate the probability of ship grounding. Cenk Sakar et al. [47] developed a method that combines fault tree and Bayesian network to evaluate the risk of ship grounding. Jiang et al. [48] employed a Bayesian network to evaluate the risk of ship grounding in the Three Gorges reservoir area, taking into account ship characteristics, organisational factors, hydrological conditions and human factors. Fu et al. [30] developed an accident graph-Bayesian network model to study the causal relationships among ship grounding accidents in the Arctic region and identify the probability of such accidents happening. Besides grounding accident records and AIS data, environmental factors like water depth, seabed topography and meteorological conditions are also utilised in the analysis of grounding risk to enhance the accuracy of the assessment. As an example, Abaei et al. [49] developed a framework to estimate the probability of ship grounding when navigating through shallow water areas, highlighting the influence of wave height on the risk of ship grounding. Likewise, Zhang et al. [29] presented a method that applied big data analysis to assess the probability of ship grounding. To accomplish this, they integrated data from AIS, meteorological observations and bathymetric surveys to evaluate the grounding risk of ro-ro passenger ships sailing in the Gulf of Finland. Yang et al. [43] developed a quantitative framework for channel grounding risk based on the empirical ship domain, employing water depth data and terrain data to evaluate the grounding risk in the waterways of the Yangtze River Estuary.

For allision incidents, Liu et al. [50] developed a probabilistic analytics method to evaluate the ship-buoy contact risk for striking ship identification at the coastal areas by combining buoy domain and bounding box models. Wu et al. [51] proposed a fuzzy logic-based ship-bridge allision warning model, using ship position, trajectory, ship-bridge distance and environmental factors as parameters. Yu et al. [52] developed a semi-quantitative risk model based on the Bayesian network and evidence reasoning approach to evaluate the allision risk between ships and offshore wind farms.

The assessment methods for static environmental risks mentioned above, while covering scenarios like grounding and allision, still have certain limitations. Most of the research focuses on risk assessment in specific static navigation environments, with the methods applicable to risks in particular geographic settings. This limitation means that the models require adjustment or redevelopment when applied to other geographic environments, constraining their generalisability. Most of the models still depend on traditional methods like statistics, fault trees, and Bayesian networks, and are unable to handle highly dynamic navigation environments. Furthermore, there is a lack of effective quantitative standards to uniformly evaluate the overall level of static environmental risk across different types of static risk sources. Consequently, these methods are challenging to provide a basis for path planning and collision avoidance decision-making.

2.3. Navigation risk fusion

The ship navigation system is a complex system involving real-time interactions between humans, ships, and the surrounding environment. Different risk factors influence each other and give rise to multi-source and heterogeneous risks. Some research scholars have investigated the interrelationships between accident causes using coupling analysis methods. Fan et al. [23] proposed a framework for examining the coupling effects in the operational modes of maritime autonomous surface ships. Zhang et al. [24] investigated the problem of human-organisation factors risk coupling in maritime pilotage by using the human factors analysis and classification system and the system dynamics method. Zhou et al. [22] built a three-hierarchy Bayesian network to assess the holistic container shipping risk, which includes 28 root risks identified by the PESTLE framework. Furthermore, some

research has focused on the fusion methods for multi-source navigation risks. Chen et al. [11] developed a risk warning method based on the probability of ship domain overlap for multi-ship encounter scenarios, which enabled the quantification of the overall risk in multi-ship encounters. Yang et al. [43] proposed a weighted risk fusion formula to conduct a holistic quantitative assessment of multi-source grounding risks in ship navigation.

The aforementioned methods effectively analyse both the coupling relationships of specific risk factors and the risks in multi-ship encounters. However, they lack a comprehensive framework for understanding maritime risks, particularly regarding their multi-source and heterogeneous nature during navigation. This limitation calls for a more integrated risk assessment approach. Existing studies primarily focus on isolated risk assessments, failing to capture the interactive effects among multiple risk sources in complex waterways. This limitation hinders the comprehensive understanding of concurrent maritime hazards. Therefore, a systematic framework is urgently needed to address two critical aspects: analysing dynamic risk interactions in changing environments and conducting a holistic assessment of multi-source, heterogeneous risks.

2.4. Research gaps

The literature review reveals three major developments in maritime risk assessment: dynamic target risk assessment has progressed from index-based to safety boundary methods, static environmental risk research has expanded to incorporate multiple analytical approaches for specific scenarios, and risk fusion studies have begun addressing the interconnected nature of maritime risks. These advances reflect the field's evolution toward more sophisticated and integrated approaches. However, a comprehensive framework capable of effectively handling heterogeneous risks while maintaining practical utility remains a significant challenge in maritime navigation safety. The research on navigation risk assessment is categorised based on different study subjects, as shown in Table 1. Despite advancements in maritime navigation risk assessment, several critical gaps remain that this study aims to address:

(1) Inadequate integration of multi-source risks: Current methodologies predominantly assess individual risk types in isolation, thereby failing to comprehensively capture the interactive and cumulative effects of heterogeneous risks encountered during maritime navigation. This limitation constrains the understanding of complex risk landscapes inherent in dynamic maritime environments.
(2) Oversimplified risk assessment models: Many existing risk assessment frameworks rely on idealised assumptions and overly simplified parameters, often neglecting critical variables such as ship size and operational behaviour. Consequently, these models may yield inaccurate and potentially misleading evaluations of navigational risks in real-world scenarios.
(3) Insufficient consideration of human factors: The integration of human decision-making processes into risk assessment frameworks remains inadequate. Current approaches frequently overlook the varying sensitivities of ship officers to different types of navigational hazards, thereby failing to account for the complexities of human cognition in automated navigation systems.
(4) Limited early warning capabilities: Existing risk assessment tools often lack robust mechanisms for providing timely and effective risk warnings. This deficiency impedes proactive decision-making by maritime operators, ultimately increasing the likelihood of maritime accidents and compromising safety.

These identified gaps elucidate the necessity for a more comprehensive and integrated approach to maritime risk assessment, which this study seeks to address through its innovative framework and methodologies.

3. The proposed methodology

This study presents a comprehensive framework for quantifying and

Table 1
Comparison of relevant navigation risk assessment methods.

Research subjects	Reference	Method	Data	Risk integration	Support collision/ allision avoidance decision-making
DT	Zhao et al. [34]	evidential reasoning	-	N	Y
DT	Bukhari et al. [35]	fuzzy inference system	AIS	N	Y
DT	Ahn et al. [36]	fuzzy inference system	expert knowledge	N	Y
DT	Li et al. [37]	D-S evidence theory	AIS	N	Y
DT	Goerlandt et al. [38]	fuzzy expert system	expert knowledge	N	Y
DT	Liu et al. [39]	cooperative game theory	AIS	Y	Y
DT	Ma et al. [40]	Monte Carlo simulation & Bayesian network	AIS	N	N
DT	Altan [42]	collision diameter	AIS, current	N	Y
DT	Chen et al. [11]	ship domain	AIS	Y	Y
DT	Silveira et al. [15]	ship domain	AIS	N	Y
SE	Yang et al. [43]	ship domian	AIS, water depth, channel	Y	Y
SE	Youssef et al. [45]	statistical analysis	accident report	N	N
SE	Sakar et al. [47]	fault tree analysis & Bayesian network	accident report	Y	N
SE	Jiang et al. [48]	Bayesian network	accident report	Y	N
SE	Abaei et al. [49]	Bayesian network & the hydrodynamic model	ship geometry data	N	N
SE	Liu et al. [50]	ship domian	AIS, bouy data, accident report	Y	Y
SE	Wu et al. [51]	ship domain & IF-THEN	AIS, wind, sea sate	N	Y
SE	Yu et al. [52]	evidential reasoning & Bayesian network	AIS	Y	N
SE	Zhang et al. [29]	Dynamic time warping & Douglas Peucker	AIS, water depth	Y	Y
DT & SE	Khaled et al. [46]	Bayesian network	AIS	Y	N
DT & SE	Bakdi et al. [53]	ship domain	AIS, water depth	N	N
DT & SE	The proposed framework	ship domain	AIS, water depth, traffic separation schemes (TSS)	Y	Y

DT: dynamic target risk.
SE: static environmental risk.

fusing multi-source heterogeneous navigation risks aimed at providing a detailed mapping of overall risk levels in ship navigation. The framework is structured into four key components:

Section 3.1 details the construction of a spatiotemporal risk monitoring domain model, which integrates risk monitoring with restricted areas using historical AIS data mining techniques. This module establishes the foundation for monitoring navigational risks and identifying forbidden areas. Section 3.2 introduces functions for evaluating heterogeneous navigation risks, focusing on both dynamic target risks and static environmental risks. It addresses the types of risks ships encounter during navigation, enabling a more precise risk assessment. Section 3.3 develops quantification methods for these risks, analysing dynamic target risks from temporal and spatial perspectives, while also categorising and assessing static environmental risks. This module provides the necessary tools to quantify risk levels based on ship movements and environmental changes. Section 3.4 presents a multi-source heterogeneous navigation risk fusion method, which is aligned with the principles of officers' risk perception. It incorporates real ship trajectories across various scenarios such as crossing, overtaking, and multi-ship encounters, ultimately offering a comprehensive risk analysis.

In summary, these sections collectively establish a cohesive methodology for risk monitoring and evaluation, with each submodule contributing to a comprehensive risk assessment framework. The submodules are interlinked, starting from risk identification and evaluation (Sections 3.1 and 3.2), to quantification (Section 3.3), and finally risk fusion and analysis (Section 3.4). Together, they form an integrated approach to heterogeneous navigation risk assessment, with each part playing a crucial role in refining the overall model. The entire framework is illustrated in Fig. 1.

3.1. Spatiotemporal risk monitoring domain model

3.1.1. Extraction of relative position relationships between ships

The study uses historical trajectory data to analyse ships' relative positions over time, capturing their spatiotemporal distribution patterns in target waters. This analysis reveals principles that guide safe navigation distances. Additionally, the Closest Point of Approach (CPA), a key metric for describing ship encounters, offers valuable insights into determining safe distances between ships. Therefore, relative positions and CPAs are systematically used in this study to quantify safe navigation distances.

To determine the relative positions between ships, both the relative distance and bearing are calculated. First, a set of Maritime Mobile Service Identity (MMSI) numbers is generated from the dataset containing all ship trajectories. Then, this MMSI set is traversed to identify the 'own ships.' Using the timestamps in each own ship's AIS data, other ships with different MMSI numbers present at the same moment are identified.

Let the geographic coordinates of the own ship and target ship be represented as (lon_{os}, lat_{os}) and (lon_{ts}, lat_{ts}), respectively. The relative

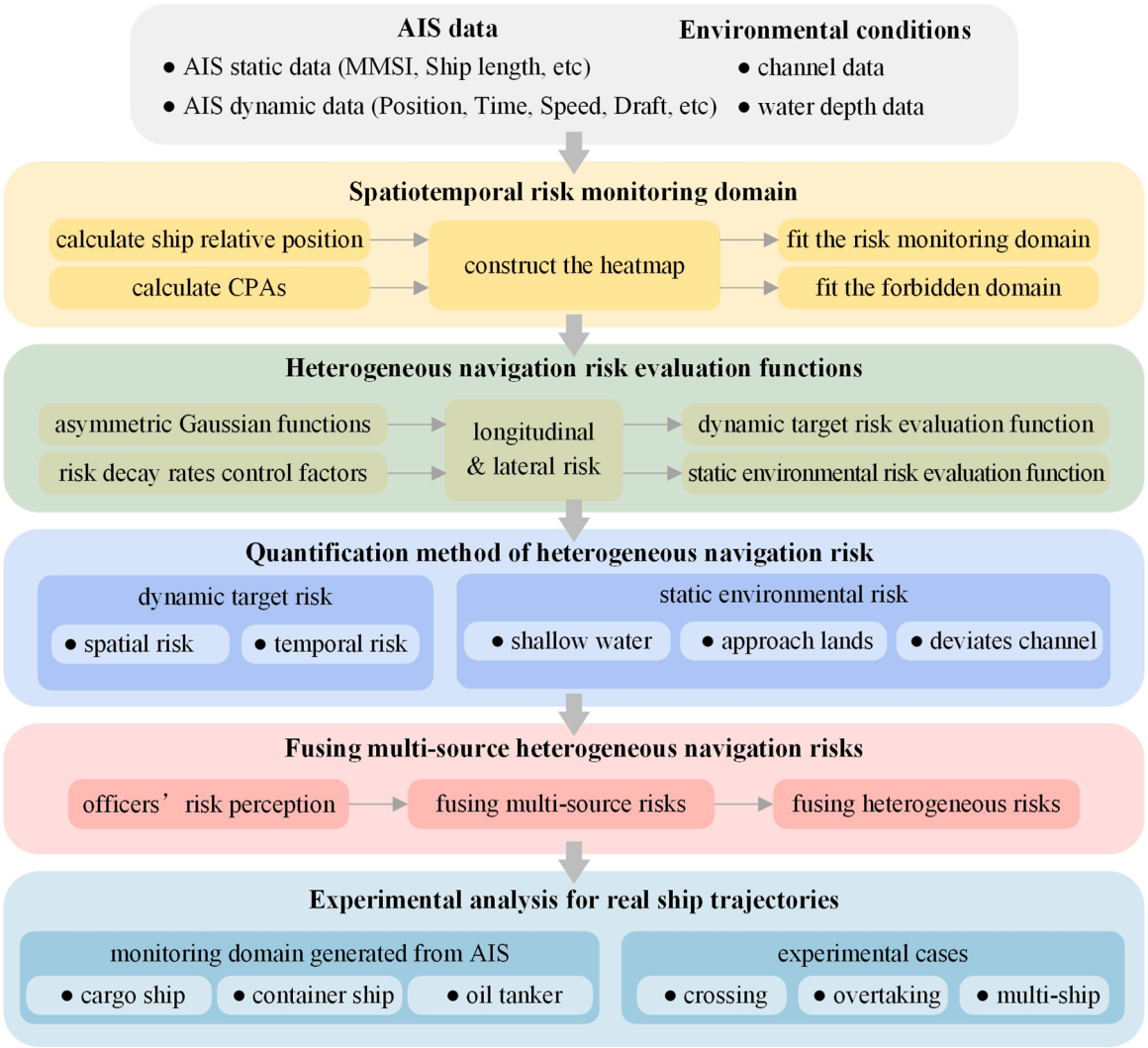

Fig. 1. Framework of quantifying and fusing multi-source heterogeneous navigation risks.

distance and bearing between these two ships are then calculated using Eqs. (1) and (2).

$$D_{relative} = \sqrt{(lon_{ts} - lon_{os})^2 + (lat_{ts} - lat_{os})^2} \tag{1}$$

where $D_{relative}$ represents the relative distance between the target ship and the own ship. lon_{os} and lat_{os} are the longitude and latitude coordinates of the own ship, respectively, while lon_{ts} and lat_{ts} stand for the longitude and latitude coordinates of the target ship, respectively.

$$B_{relative} = arctan((lon_{ts} - lon_{os}) / (lat_{ts} - lat_{os})) + \Delta B \tag{2}$$

The value of ΔB is calculated according to Eq. (3).

$$\Delta B = \begin{cases} 0^{\circ} & (lon_{ts} - lon_{os}) \geq 0, (lat_{ts} - lat_{os}) \geq 0 \\ 180^{\circ} & (lat_{ts} - lat_{os}) < 0 \\ 360^{\circ} & (lon_{ts} - lon_{os}) < 0, (lat_{ts} - lat_{os}) \geq 0 \end{cases} \tag{3}$$

Calculating the distance between ships is challenging due to their positions in a spherical coordinate system. To address this, the geographic coordinates are converted into Cartesian coordinates using the Mercator projection. This transformation follows Eqs. (4)–(7).

$$r_0 = \left(a\_earth \Big/ \sqrt{1 - e^2 * sin^2\varphi_0}\right) * \cos\varphi_0 \tag{4}$$

$$q = ln\, tan(\pi/4 + lat/2) + 0.5 * e * \ln((1 - e * \sin(lat)) / (1 + e * \sin(lat))) \tag{5}$$

$$lon_{cart} = lon * r_0 \tag{6}$$

$$lat_{cart} = lat * r_0 \tag{7}$$

where r_0 denotes the radius at the standard parallel, and φ_0 is the standard latitude used in the Mercator projection. a_earth represents the semi-major axis of Earth's ellipsoid, e designates Earth's first eccentricity, and q is defined as the isometric latitude. The terms lon_{cart} and lat_{cart} refer to the longitude and latitude of the ship in the Cartesian coordinate system, respectively.

Therefore, after the coordinate system transformation, Eqs. (1) and (2) are updated to Eqs. (8) and (9).

$$D_{relative} = \sqrt{\left(lon_{ts}^{cart} - lon_{os}^{cart}\right)^2 + \left(lat_{ts}^{cart} - lat_{os}^{cart}\right)^2} \tag{8}$$

$$B_{relative} = arctan\left(\left(lon_{ts}^{cart} - lon_{os}^{cart}\right) / \left(lat_{ts}^{cart} - lat_{os}^{cart}\right)\right) + \alpha \tag{9}$$

where lon_{os}^{cart} and lat_{os}^{cart} represent the longitude and latitude of the own ship in the Cartesian coordinate system, respectively. Similarly, lon_{ts}^{cart} and lat_{ts}^{cart} indicate the longitude and latitude of the target ship in the Cartesian coordinate system, respectively.

After completing the above steps, the relative position data of the own ship is obtained and non-dimensionalised by the ship's length. Then, multiple sets of coordinate points are extracted by traversing the MMSI set. These relative positions are visualised using a heatmap, which is discretised into grids of 0.2 × 0.2 times the ship length. The heatmap has a height of 16 times the ship length and a width of 10 times the ship length.

In this study, the CPA is defined as the point where the distance between two ships is minimised during an encounter. After calculating the relative position data between ships, the minimum distance is identified as the CPA. The detailed processing flow is shown in Table 2. Finally, the series of CPAs are visualised on a heatmap.

3.1.2. Fit the spatiotemporal risk monitoring domain

After generating the heatmaps for relative position relationships and CPAs, an approximately elliptical low-density area is observed near the centre of the ships. As shown in Fig. 2, the low-density area in the relative position relationship heatmap is larger than that in the CPA heatmap.

To extract the features of two low-density ship domains, the boundaries of the two domains are fitted using the least squares method according to Eq. (10).

$$((x - x_c * L)/a * L)^2 + ((y - y_c * L)/b * L)^2 = 1 \tag{10}$$

where (x, y) represents the coordinates of points on the fitted boundary of the ship domain. L is the ship's length in metres, while a and b are the semi-major and semi-minor axes of the fitted ship domain, respectively. (x_c, y_c) denotes the centre point of the fitted ship domain.

A larger domain boundary can be defined as the navigation risk monitoring boundary. As shown in Fig. 3(a), if obstacles, non-navigable waters, or the domains of other ships intrude into the own ship's risk monitoring domain, a navigation risk is identified. Conversely, a smaller domain boundary serves as the ship's forbidden domain. As illustrated in Fig. 3(b), if obstacles, non-navigable waters, or the domains of other ships enter the own ship's forbidden domain, the navigation risk is considered excessively high.

3.2. Heterogeneous navigation risk evaluation functions

During navigation, ships engage in complex real-time interactions with the external environment, which give rise to multi-source and heterogeneous risks. Multi-source risks refer to scenarios where risk originates from multiple sources. For instance, in multi-ship encounter situations, interactions with multiple target ships may generate multiple collision risk factors. Heterogeneous risks, on the other hand, highlight the diversity of risk types. For example, in narrow waterways, ships not only face collision risks with target ships but also encounter risks such as straying off the navigational channel or grounding. These multi-source and heterogeneous risks pose significant challenges to maritime safety.

This study examines the risks arising from the real-time interactions between ships and their external environment during navigation. It particularly emphasises the spatiotemporal interactions between ships, static navigational environments, and dynamic obstacles. The goal is to uncover the underlying mechanisms of these heterogeneous navigation risks. To this end, the study classifies them into two categories: dynamic target risks and static environmental risks.

Dynamic target risks arise when a ship encounters other moving targets (e.g., other ships) during navigation. These risks stem from the relative motion between the ship and dynamic targets, as well as potential conflicts in their navigational paths, which could lead to severe accidents such as collisions.

Static environmental risks, on the other hand, result from a ship's interaction with fixed or relatively stationary environmental factors (e.g., channel topography, meteorological, and hydrological conditions)

Table 2
CPA calculation process.

CPA calculation process
Input:$MMSI_{set}$, $D - list_{relative}$;$MMSI_{set}$ is the set containing the MMSI numbers of all ships, and $D - list_{relative}$ represents the list containing the relative position distances of all ships.
Output:$MD - list_{relative}$: This is the list containing the distances of the CPA for all ships.
1:for i in $MMSI_{set}$:
2: $MD_i = min(D - list_{relative}^{i})$
3: $MD - list_{relative}$.append(MD_i)
4:return $MD - list_{relative}$

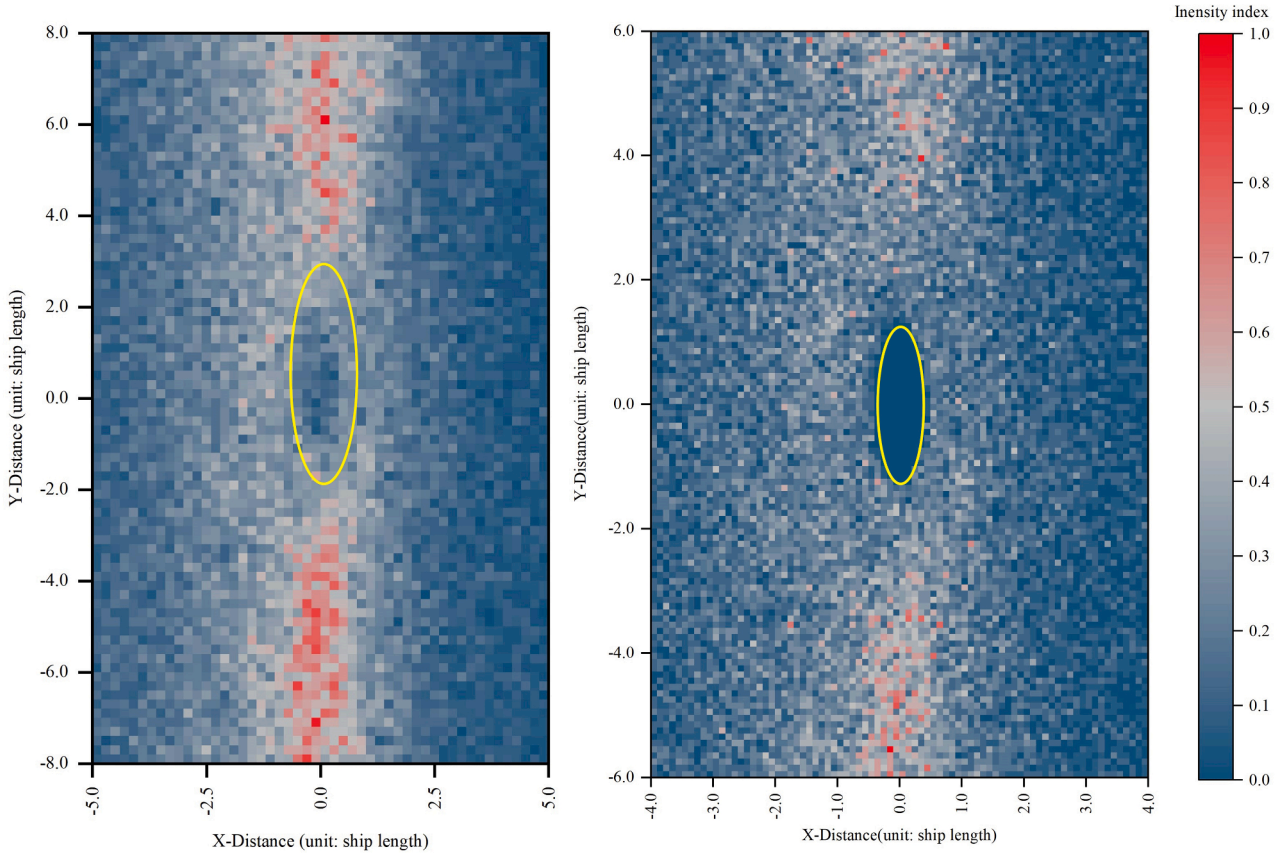

Fig. 2. Comparison of relative position and CPA heatmaps.

during navigation. These risks often arise from the complexity and unpredictability of the environment, potentially leading to accidents such as grounding, reefing, or loss of control under adverse weather conditions.

After modelling both the risk monitoring and forbidden domains, the framework for quantifying navigational risks for ships is established. However, to derive specific values for different types of navigational risks, it is necessary to define spatial risk functions that represent the risk levels. Yang et al. [43] developed grounding evaluation functions that illustrate the distribution of risks from both longitudinal and lateral perspectives. They used an asymmetric Gaussian function to capture the sensitivity of risks from different directions. Referring to these functions, an asymmetric Gaussian function is adopted to construct the heterogeneous navigation risk evaluation functions.

First, four semi-axes of the risk monitoring domain are defined as $R_{i,f}$, $R_{i,a}$, $R_{i,s}$, and $R_{i,p}$. Here, $R_{i,f}$ and $R_{i,a}$ represent the forward and after semi-axes of ship i's longitudinal risk monitoring domain, respectively, while $R_{i,s}$ and $R_{i,p}$ indicate the starboard and port semi-axes of ship i's lateral risk monitoring domain. These semi-axes are calculated according to Eq. (11).

$$\begin{cases} R_{i,f} = (b + y_c) * L \\ R_{i,a} = (b - y_c) * L \\ R_{i,s} = (a + x_c) * L \\ R_{i,p} = (a - x_c) * L \end{cases} \tag{11}$$

where the parameters are the same as those in Eq. (10).

The dynamic target risk evaluation functions are constructed as the product of longitudinal and lateral dynamic target risk evaluation functions, decaying along the four semi-axes. The decay rates are controlled by the parameters $R_{i,f}$, $R_{i,a}$, $R_{i,s}$ and $R_{i,p}$. In general, officers tend to prioritise dynamic target risks over static environmental risks [54]. Therefore, the decay rates of the dynamic target risk evaluation functions are uniformly set to low values.

To evaluate the longitudinal dynamic target risk for ship i, the function $DSR_{i,Lon}(y)$ is calculated as specified in Eq. (12). Parameters $R_{i,f}$ and $R_{i,a}$ are key factors that determine the decay rate of $DSR_{i,Lon}(y)$.

$$DSR_{i,Lon}(y) = exp\Big(- \big(y\alpha / \big((1 + sign(y))R_{i,f} - (1 - sign(y))R_{i,a}\big)\big)^2 \Big) \tag{12}$$

$$\alpha = (ln(\,1/r_0))^{0.5}, r_0 = 0.5 \tag{13}$$

$$sign(x) = \begin{cases} 1, \ if \ x \geq 0 \\ -1, \ if \ x < 0 \end{cases} \tag{14}$$

The lateral dynamic target risk evaluation function, $DSR_{i,Lat(x)}$, follows a similar structure to the longitudinal dynamic target risk evaluation function $DSR_{i,Lon(y)}$. Parameters $R_{i,s}$ and $R_{i,p}$ define the right and left semi-axes of the domain, respectively, and control the decay rate of $DSR_{i,Lat(x)}$. This function is calculated according to Eq. (15).

$$DSR_{i,Lat}(x) = exp\Big(- \big(x\alpha / \big((1 + sign(x))R_{i,s} - (1 - sign(x))R_{i,p}\big)\big)^2 \Big) \tag{15}$$

For a given ship i, the dynamic target risk is assumed to be the product of its longitudinal and lateral dynamic target risks. The specific risk value is determined according to Eq. (16). The spatial distribution of the dynamic target risk evaluation function is shown in Fig. 4(a).

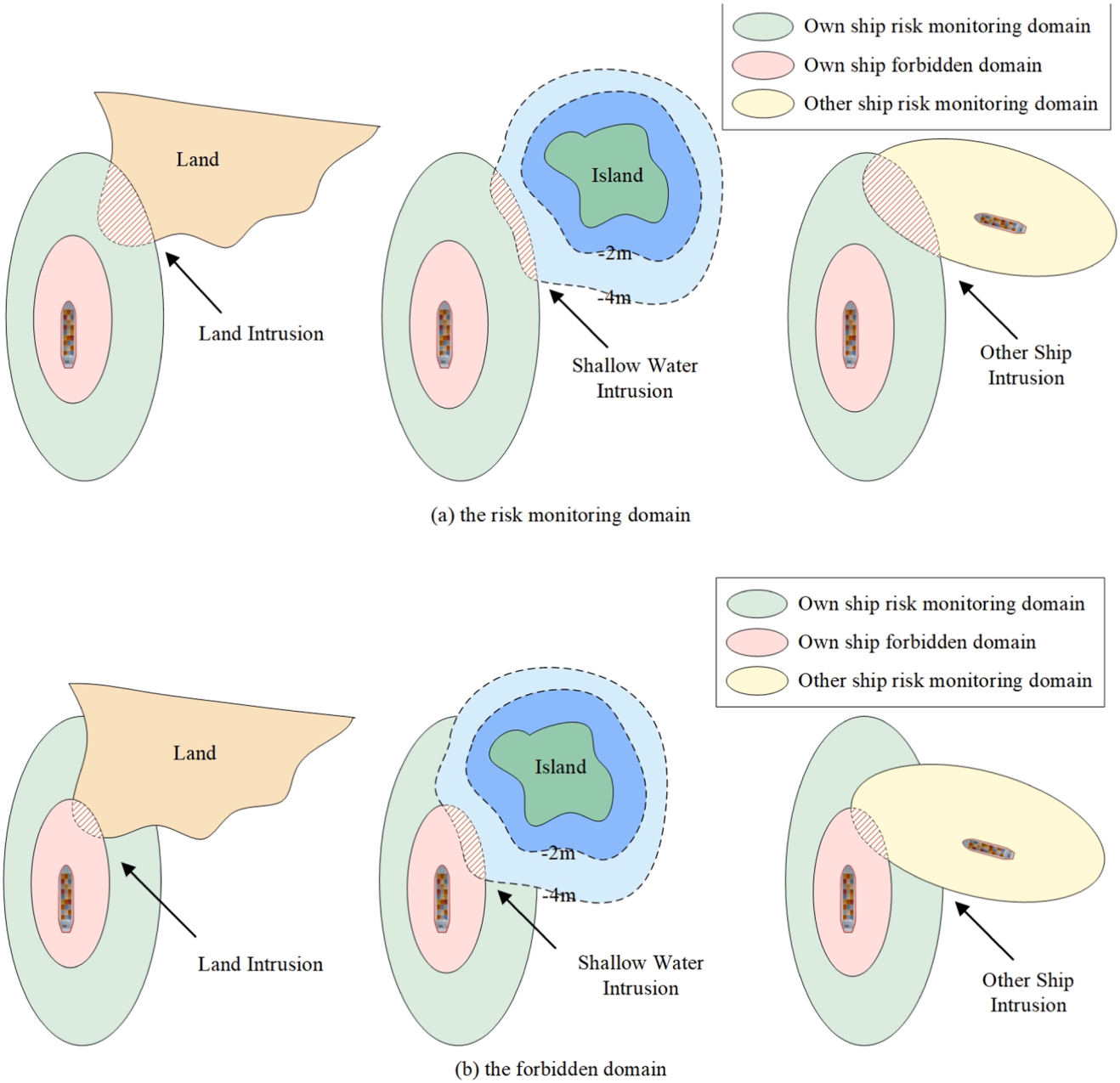

Fig. 3. Spatiotemporal risk monitoring domain model.

$$DSR_i(x,y) = DSR_{i,Lon}(y) * DSR_{i,Lon}(x)$$
$$= exp\Big(\big(- \big(y\alpha/\big((1+sign(y))R_{i,f} + (1-sign(y)R_{i,a})\big)\big)^2\big) + \big($$
$$- \big(x\alpha/\big((1+sign(x))R_{i,f} - (1-sign(x))R_{i,a})\big)\big)^2\big)\Big) \tag{16}$$

The grounding risk evaluation functions proposed by Yang et al. [43] are adopted as the static environmental risk evaluation function. This grounding risk model assesses risk in navigational waters by calculating the overlapping areas between empirical ship domains and non-navigable waters, aligning with the evaluation approach of the proposed model.

For a given ship i, its static environmental risk is calculated according to Eq. (17). The spatial distribution of the static environmental risk evaluation function is shown in Fig. 4(b).

$$SR_i(x,y) = SR_{i,Lon}(y) \times SR_{i,Lat}(x)$$
$$= exp\Big(\big($$
$$- \big(2y\alpha/\big(2*(1+sign(y))R_{i,f} + (1-sign(y)R_{i,a})\big)\big)^2\big) + \big($$
$$- \big(2x\alpha/\big((1+sign(x))R_{i,f} - (1-sign(x))R_{i,a})\big)\big)^2\big)\Big) \tag{17}$$

To further analyse the differences between the static environmental risk function and the dynamic target risk function, their profiles along the Y-axis and X-axis were plotted. As shown in Fig. 5(a), both functions decay at the same rate along the positive Y-axis; however, the dynamic target risk function decays more slowly in the negative Y-axis direction. This indicates that, at equivalent positions on the negative half of the Y-axis, the dynamic target risk is assessed to be higher than the static environmental risk. Similarly, Fig. 5(b) shows that the dynamic target risk function also decays more slowly along the X-axis, suggesting that at

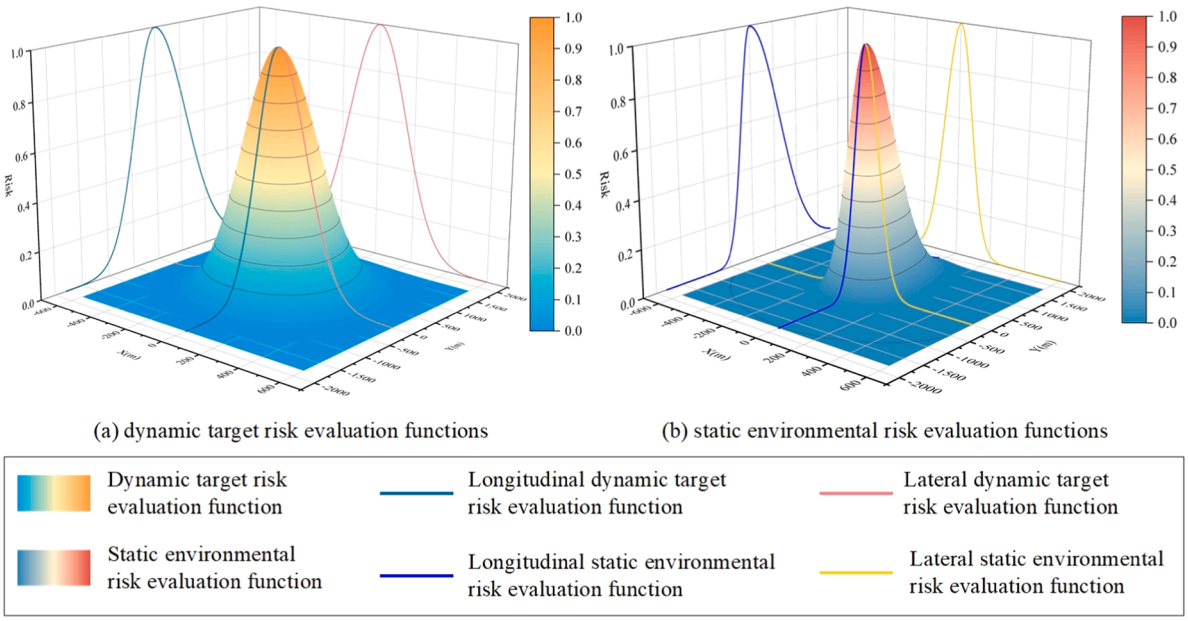

Fig. 4. The spatial distribution of risk evaluation functions (ship length of 150 m).

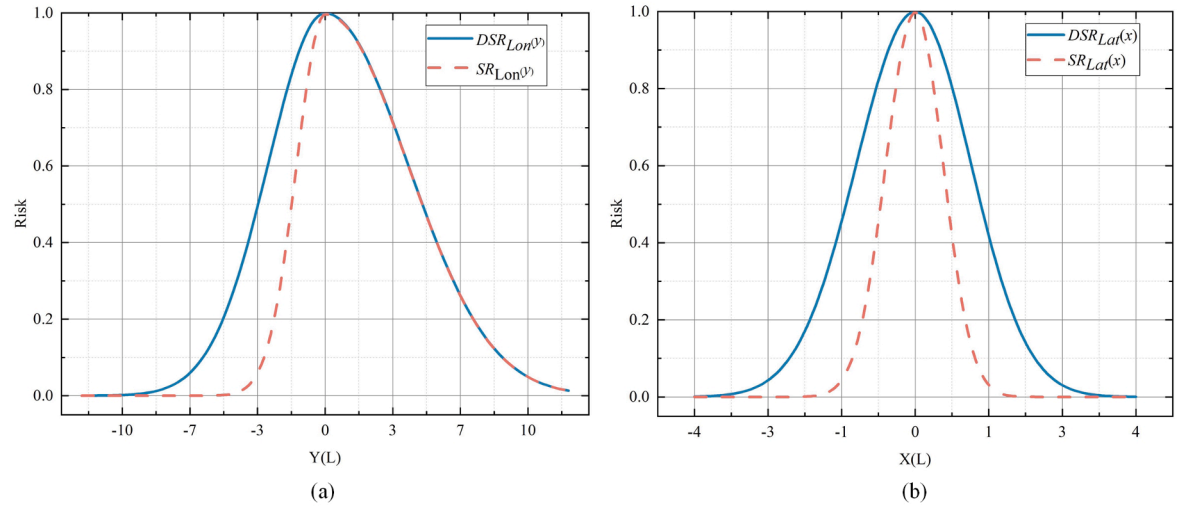

Fig. 5. Risk evaluation function: (a) Longitudinal dynamic target risk evaluation function & Longitudinal static environmental risk evaluation function; (b) Lateral dynamic target risk evaluation function & Lateral static environmental risk evaluation function.

corresponding positions on the X-axis, the dynamic target risk is higher than the static environmental risk. This is consistent with the higher sensitivity of officers to dynamic target risks, as noted in [54].

3.3. Quantification method of heterogeneous navigation risk

This study considers two main types of navigation risks: dynamic target risks and static environmental risks. The former addresses collision risks between ships based on their relative positions and motion trends, while the latter accounts for risks from shallow waters, land proximity, and channel deviation, which are evaluated through the spatiotemporal relationship between ships and these static hazards. The following sections present a comprehensive methodology for quantifying these identified risks.

3.3.1. Quantification method of dynamic target risk

Heterogeneous navigation risks are subdivided into dynamic target risks and static environmental risks. Dynamic target risk refers to the risk arising from an encounter scenario between the own ship and a target ship. This type of risk results from the interaction between two or more dynamic entities. Therefore, it must be quantified from both a spatial and a temporal perspective. The spatial perspective is based on the relative positions of the ships, while the temporal perspective considers the relative motion trends of the ships.

From a spatial perspective, risk is determined when the spatiotemporal risk monitoring domain of the target ship overlaps with that of the own ship. For example, in Fig. 6(a), ship B's domain intrudes into ship A's domain, creating a risk between ships A and B, while there is no overlap between ships A and C, indicating no risk between them. To quantify the dynamic target risk, the integral of the dynamic target risk function is calculated over the overlapping area. However, the result may be greater than 1, making direct application for risk warnings difficult. Thus, the results need to be normalised. The overlapping area of the two ships' domains is labelled as A_i (red diagonal lines in Fig. 6 (b)), and the integral over this area is DR_i. The centroid of A_i is connected to the ship's centre, forming a translation line (green dashed

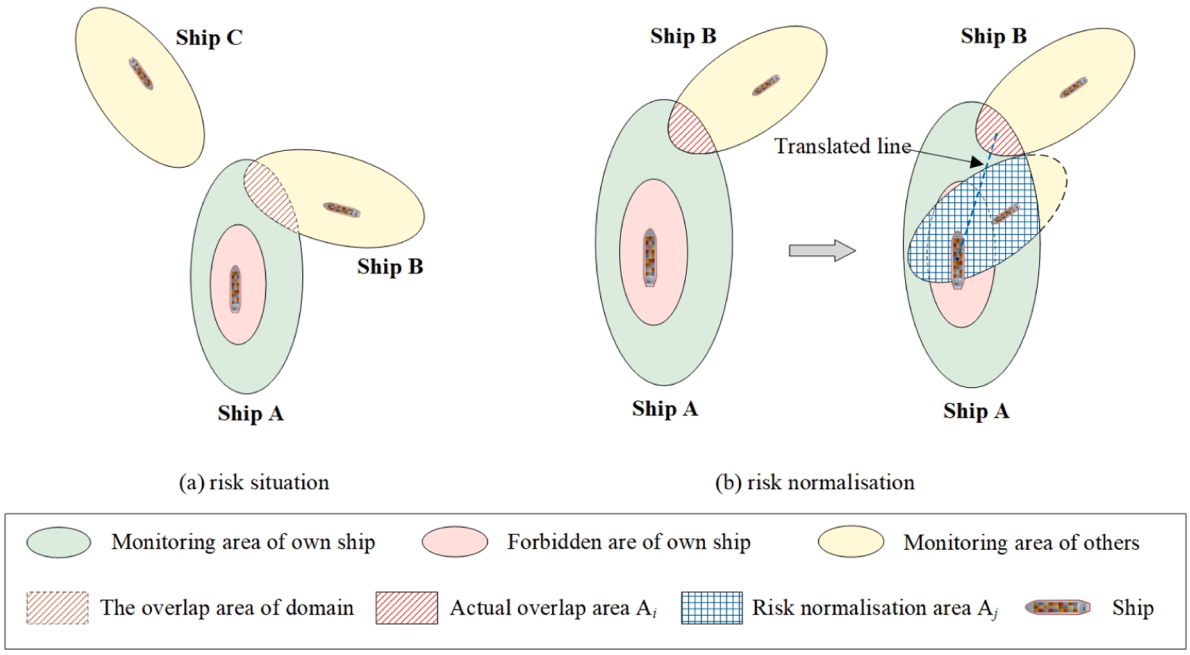

Fig. 6. Schematic diagram of the dynamic target risk scenario.

line). Ship B is then moved along this line until its domain touches the forbidden boundary of ship A. The new overlapping area is labelled A_j (blue squares in Fig. 6(b)), and the integral over this area is DR_j. Finally, the dynamic target risk is calculated as the ratio of DR_i to R_j, expressed as $DR_c = DR_i/DR_j$.

From a temporal perspective, dynamic target risk must be quantified based on the motion trends between ships. Suppose there is an own ship (ship A) and a target ship (ship B). As shown in Fig. 7, the coordinates of the two ships at time t are (x_{at}, y_{at}) and (x_{bt}, y_{bt}), respectively. The relative position vector between the ships at time t can be calculated using Eq. (18).

$$\vec{BA}_t = \vec{OB}_t - \vec{OA}_t = (x_{bt} - x_{at}, y_{bt} - y_{at}) \tag{18}$$

where $\overrightarrow{OA_t}$ is the position vector of ship A at time t, $\overrightarrow{OB_t}$ represents the position vector of ship B at time t, and $\overrightarrow{BA_t}$ denotes the relative position vector between ship A and ship B.

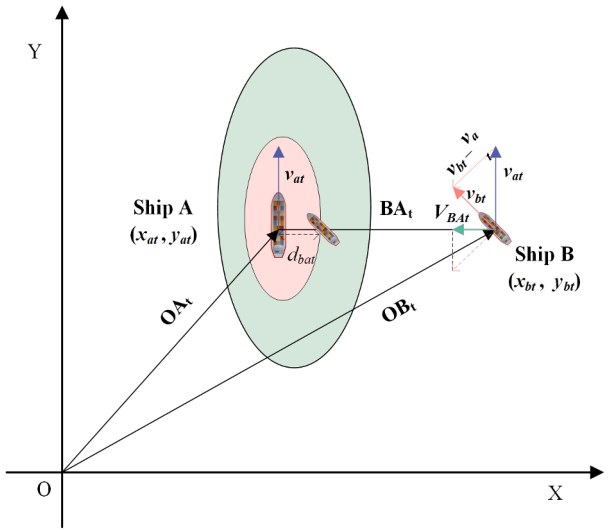

Fig. 7. Schematic diagram of collision time margin calculation.

The velocity vector coordinates of the ships at time t are calculated using Eq. (19):

$$\vec{v} = (v * sin\alpha, v * cos\alpha) \tag{19}$$

where $\vec{v}$ stands for the velocity vector of the ship, v is the magnitude of the ship's speed, and α represents the ship's heading.

As shown in Fig. 7, the time margin for a potential collision is calculated by dividing the distance from the target ship (ship B) to the forbidden boundary of the own ship (ship A) under the current motion state by the velocity component of the other ship in that direction. The time margin can be calculated using Eq. (20).

$$T_m = \frac{|\vec{BA}_t| - d_{bat}}{\vec{V}_{BAt}} \tag{20}$$

where T_m represents the time margin; $\vec{BA}_t$ is the relative position vector between ship A and ship B; and $\vec{V}_{BAt}$ stands for the projection of the relative velocity vector between ship A and ship B onto $\vec{BA}_t$ at time t, calculated using Eq. (21). The term d_{bat} denotes the distance between ship B and the forbidden boundary of ship A when ship B is travelling towards it under the current motion state.

$$\vec{V}_{BAt} = \vec{v}_{BAt} \cdot \vec{BA}_t \Big/ \left|\vec{BA}_t\right| \tag{21}$$

where $\vec{v}_{BAt}$ designates the relative velocity vector between ship A and ship B, calculated using Eq. (22).

$$\vec{v}_{BAt} = \vec{v}_{Bt} - \vec{v}_{At} = (\vec{v}_{bt} * sin\alpha_{bt} - \vec{v}_{at} * sin\alpha_{at}, \vec{v}_{bt} * cos\alpha_{bt} - \vec{v}_{at} * cos\alpha_{at}) \tag{22}$$

The temporal margin (T_m) characterises the relative motion states between ships. When T_m is negative, the ships are moving apart. A zero T_m indicates that ships have reached their closest relative distance. Conversely, a positive T_m suggests that ships are approaching each other. From a temporal perspective, the collision risk exhibits an inverse relationship with the time margin. To quantify this risk level, a power function is employed to evaluate the dynamic target risk at time t based on the time margin. The mathematical representation of the dynamic

target risk value from the temporal perspective is expressed in Eq. (23).

$$\begin{cases} DRT = 0, \ \rightarrow V_{BAt} \leq 0 \\ DRT = \ 1 \Big/ (1 + (k * T_m)^n), \ \rightarrow V_{BAt} > 0, \left| \vec{BA}_t \right| > d_{bat} \\ DRT = 1, \ \rightarrow V_{BAt} > 0, \left| \vec{BA}_t \right| \leq d_{bat} \end{cases} \tag{23}$$

where DRT represents the dynamic target risk value of the ship from a temporal perspective at time t; $\vec{V}_{BAt}$ denotes the projection of the relative velocity vector between ships A and B at time t onto $\vec{BA}_t$; $\vec{BA}_t$ indicates the relative position vector between ships A and B; d_{bat} signifies the distance between ship B and ship A's forbidden boundary, measured along ship B's current trajectory; k and n are empirical parameters controlling the power function's shape and decay rate, respectively, determined through expert knowledge, with k set to 0.02 and n set to 2 in this study.

Following the acquisition of dynamic target risk results from both spatial and temporal perspectives, a comprehensive spatiotemporal risk quantification becomes essential. Maritime observations indicate that officers exhibit lower sensitivity to velocity variations during actual navigation, primarily focusing on inter-ship distance variations for risk assessment. The spatial perspective of dynamic target risk, therefore, carries greater significance in navigational decision-making compared to its temporal counterpart. The temporal perspective serves as a complementary indicator to the spatial risk assessment. Based on these considerations, the risk fusion methodology proposed by Chen et al. [11] has been adopted, which employs catastrophe theory to construct an integrated spatial-temporal risk fusion model. The mathematical expression is presented in Eq. (24).

$$DR_t = \left(\sqrt{DSR_t} + \sqrt[3]{DRT} \right) \Big/ 2 \tag{24}$$

where DR_t represents the comprehensive spatiotemporal dynamic target risk value at time t; DSR_t denotes the spatial dynamic target risk value at time t; DRT signifies the temporal dynamic target risk value at time t.

3.3.2. Quantification method of static environmental risk

Static environmental risk encompasses three primary components: proximity to shallow waters and reefs, approach to land, and deviation from designated channels. Maritime navigation requires maintaining safe distances from non-navigable areas whilst adhering to designated channels, which offer optimal water depth conditions and professional maintenance through dredging operations. Areas beyond these channels typically present suboptimal depth conditions due to geographical constraints and other factors, thereby elevating navigational risks for deviating ships. The quantification of static environmental risk utilises the spatiotemporal relationship between ships, non-navigable waters, and channels. This methodology involves integrating the static environmental risk function across the intersection of the ship's domain with non-navigable waters, whilst channel deviation risk is computed through the integration of the risk function over areas where the ship's domain extends beyond channel boundaries.

Static environmental risk assessment is conducted based on diverse environmental scenarios. As illustrated in Fig. 8, ships A, B and C are located within the navigational channel. Ship B's risk monitoring domain extends beyond the channel boundary, whilst ship C's domain intersects with shallow waters inside the channel. Consequently, ship A exhibits no static environmental risk, whereas ships B and C demonstrate significant environmental risk factors. Similarly, ships D and E, situated outside the channel, both present static environmental risks due to their respective risk monitoring domains: ship D's domain intersects with a reef area, whilst ship E's domain overlaps with terrestrial boundaries.

The quantification of static environmental risk is achieved by integrating the environmental risk evaluation function over the domain

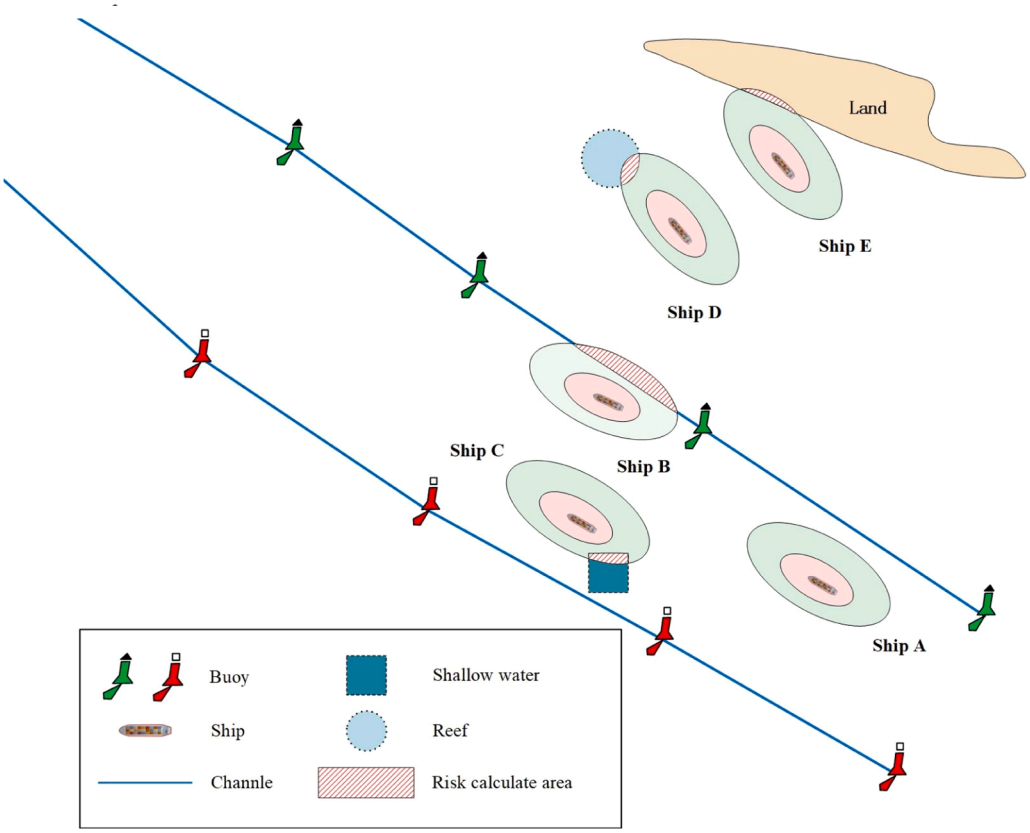

Fig. 8. Illustration of static environmental risk (within the channel: Ship A, Ship B, Ship C; outside the channel: Ship D, Ship E).

formed by the intersection between the spatiotemporal risk monitoring region and non-navigable areas. Risk normalisation is performed based on the spatial relationship between the ship and non-navigable areas within the static environment. This method corresponds to the grounding risk evaluation model established by Yang et al. [43]. Hence, detailed computational procedures are omitted for brevity. Fig. 9 illustrates the risk normalisation process for static environmental scenarios.

3.4. Multi-source heterogeneous navigation risks fusion

Multi-source heterogeneous navigation risks encompass two primary dimensions. The first dimension addresses the diversity of risk types, comprising static environmental risks (including channel deviation and proximity to non-navigable waters) and dynamic target risks (such as spatiotemporal collision risks). The second dimension pertains to the multiplicity of risk sources encountered during navigation, exemplified by simultaneous interactions between the subject ship and multiple target ships in multi-ship scenarios.

A comprehensive understanding of multi-source heterogeneous navigational risks requires systematic methodological development. The primary methodological requirements encompass two critical aspects. The first aspect involves the standardisation of quantification scales and risk dimensions through rigorous protocols. The second aspect focuses on the normalisation of risk outcomes, which serves to enhance the effectiveness of warning mechanisms.

Based on empirical observations of maritime officers' risk perception mechanisms, three fundamental principles have been synthesised for the development of the multi-source navigational risk fusion model.

(1) The maximum navigational risk value is bounded at 1; when any individual risk type reaches this threshold, the fused navigational

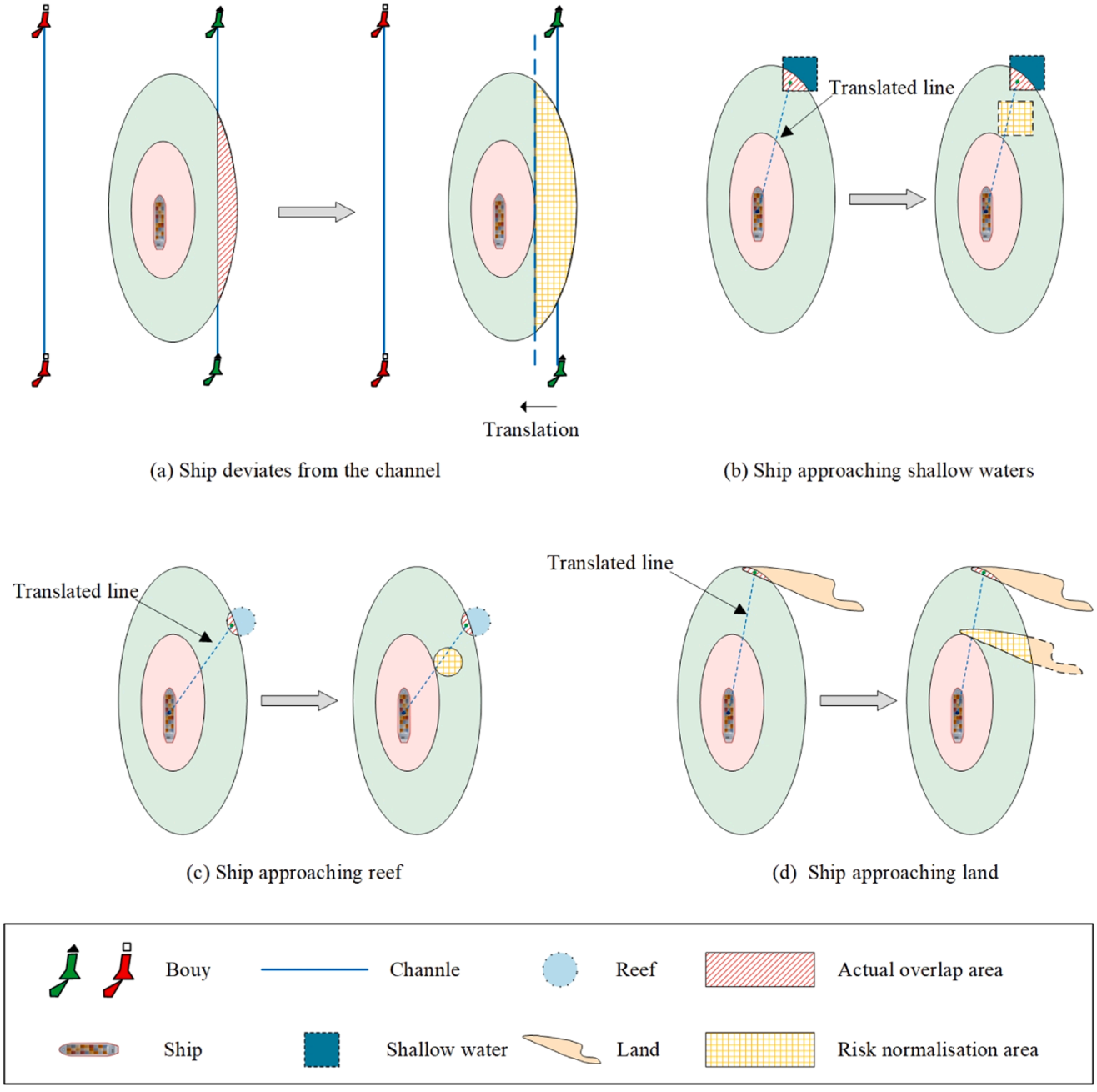

Fig. 9. Schematic diagram of static environmental risk normalisation.

risk value automatically assumes this maximum value, preventing further risk accumulation.

(2) For scenarios where individual risks remain below 1, the integrated navigational risk value must be: Less than 1; Greater than or equal to the maximum individual risk value associated with the ship and hazard source.

(3) The navigational risk value maintains a strict lower bound of 0.

The total static environmental risk for a specific ship is denoted as SR_n. This ship possesses n distinct sources of static environmental risk. Each individual risk value is represented as sr_i ($where\ i = 1, 2, \ldots, n$). These values are systematically arranged in ascending order. The computation of the ship's total static environmental risk follows Eq. (25).

$$SR_n = 1 - \prod_{i=1}^{n} (1 - sr_i) \tag{25}$$

The total dynamic target risk for a specific ship is expressed as DR_m. This ship encompasses m distinct sources of dynamic target risk. Each individual dynamic risk value is denoted as dr_i ($where\ i = 1, 2, \ldots, m$). These values are systematically arranged in ascending order. The calculation of the ship's total dynamic target risk is executed using Eq. (26).

$$DR_m = 1 - \prod_{i=1}^{m} (1 - dr_i) \tag{26}$$

Following the determination of static and dynamic risks, the comprehensive fusion value of multi-source navigational risk for the ship can be derived through Eq. (27).

$$R = \begin{cases} 1, if\ \max(SR_n, DR_m) = 1 \\ \max(SR_n, DR_m) + (1 - \max(SR_n, DR_m)) * \min(SR_n, DR_m), otherwise \end{cases} \tag{27}$$

where R denotes the fusion value of the multi-source navigational risk for the ship, SR_n stands for the total static environmental risk for the ship, and DR_m is the total dynamic target risk for the ship.

4. Experimental analysis

4.1. Experimental dataset description

Ningbo-Zhoushan Port, handling over 3500 daily ship movements, maintains its position as the world's busiest port by throughput. To address the heightened navigational risks in this high-density traffic area, the International Maritime Organization (IMO) has implemented comprehensive routing measures. The traffic management system comprises 18 TSSs, 8 precautionary zones, and a deep-water channel, as illustrated in Fig. 10(a). The study utilises AIS data from May 2019, comprising 17,487 ships with 12,132,476 trajectory points. The spatial distribution of maritime traffic is visualised through a density map in Fig. 10(b), whilst bathymetric data for non-navigable area identification is shown in Fig. 10(c).

To ensure the reliability and accuracy of our analyses, we implemented a rigorous data preprocessing protocol on the raw AIS data. This process included several key steps. First, we performed data cleaning by removing entries with speeds below 3 knots, which typically indicate non-navigational states such as mooring or construction, following established maritime practice and previous studies [43,55] .Our sensitivity analysis confirmed that varying this threshold between 2–4 knots did not significantly affect the main findings. This refinement focused our dataset on active navigation scenarios, enhancing analytical relevance. Next, we addressed gaps in static AIS data, such as missing ship dimensions and ship types, by cross-referencing established maritime databases. This static information supplementation ensured our dataset contained complete and accurate information critical for modelling navigational risks. We also excluded specific ship types, including tugboats and supply ships, which often operate close to other ships and could introduce noise into our analysis. This exclusion improved the clarity of spatiotemporal relationships in the dataset. Finally, we achieved temporal consistency across AIS timestamps by employing cubic spline interpolation, smoothing the trajectory data and filling temporal gaps for coherent ship movement analysis. These preprocessing steps resulted in a high-quality dataset that accurately reflects ship movements within the port area, thereby enhancing the reliability of subsequent analyses and the effectiveness of the empirical ship domain models used to quantify navigation risks.

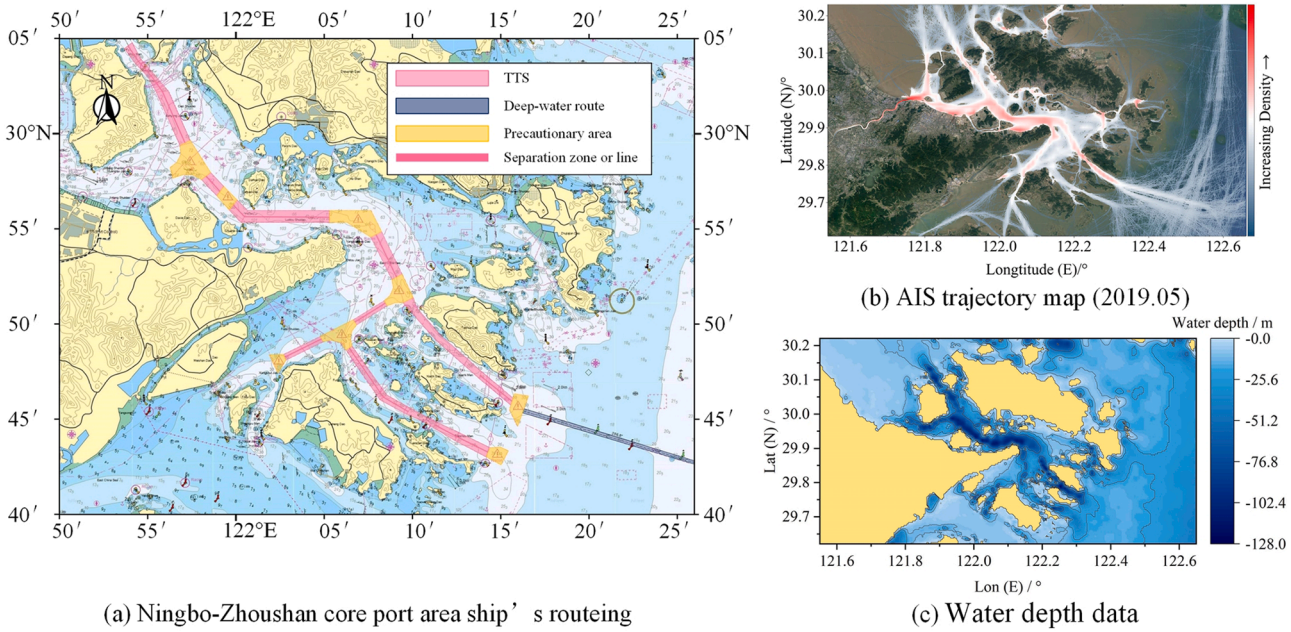

(a) Ningbo-Zhoushan core port area ship's routeing

(b) AIS trajectory map (2019.05)

(c) Water depth data

Fig. 10. Study area and related dataset.

4.2. Modelling results of the spatiotemporal risk monitoring domain

The spatiotemporal risk monitoring domain model is constructed using AIS data, following the methodology outlined in Section 3.1. The data preprocessing involves sequential steps: error removal, static information completion, exclusion of low-speed and engineering ships, and trajectory interpolation. Through iterating MMSI numbers and timestamps, the relative positions of ships and their closest points of encounter are computed, generating a heat map as shown in Fig. 11. The boundaries and forbidden areas of the ship risk monitoring domain are then derived from the heat map using the least squares method, as illustrated in Fig. 12.

In the Ningbo-Zhoushan Port waters, cargo ships predominate, whilst container ships and oil tankers are less prevalent. This distribution is reflected in the heat map of ship relative positions, where bulk carrier density significantly exceeds that of container ships and oil tankers. The fitted risk monitoring model reveals distinct characteristics across ship types, with detailed parameters presented in Table 3.

Cargo ships exhibit the smallest scale among the three ship types. Container ships present a larger model scale, with a notably extended vertical axis compared to cargo ships, likely reflecting their higher operational speeds and consequent need for greater longitudinal safety distances. Oil tankers demonstrate the largest scale, particularly in the lateral dimension, primarily due to their larger block coefficient requiring increased lateral safety margins during navigation.

To derive the ship forbidden domain model, the CPA is computed from the relative positions of ships. Following similar patterns to the risk monitoring domain model, the forbidden domain exhibits varying scales across different ship types, with detailed parameters presented in Table 4. Cargo ships demonstrate the smallest scale, whilst container ships show larger dimensions, and oil tankers present the most extensive forbidden domain. Fig. 13 illustrates the combined effects of both risk monitoring and forbidden domain models for various ship types.

4.3. Dynamic target risk case

The validation of the dynamic target risk quantification method employs analysis of representative scenarios, including crossing encounters, overtaking situations and multi-ship interactions. The assessment utilises real ship trajectories from typical encounter scenarios, incorporating key parameters: relative distance, relative speed, relative bearing, approach speed, DCPA and TCPA. Critical time points are examined to evaluate dynamic risk variations, particularly during collision avoidance manoeuvres and sudden risk transitions.

4.3.1. Dynamic target risk in ship encounter scenarios

The crossing encounter scenario involves two ships (Ship A and Ship B), with their detailed specifications presented in Table 5. According to COLREG rules, Ship A assumes the give-way responsibility whilst Ship B maintains its course as the stand-on ship. At 340 s into the encounter, Ship A executes a port turn manoeuvre, successfully passing astern of Ship B. The encounter trajectories and parameter variations are

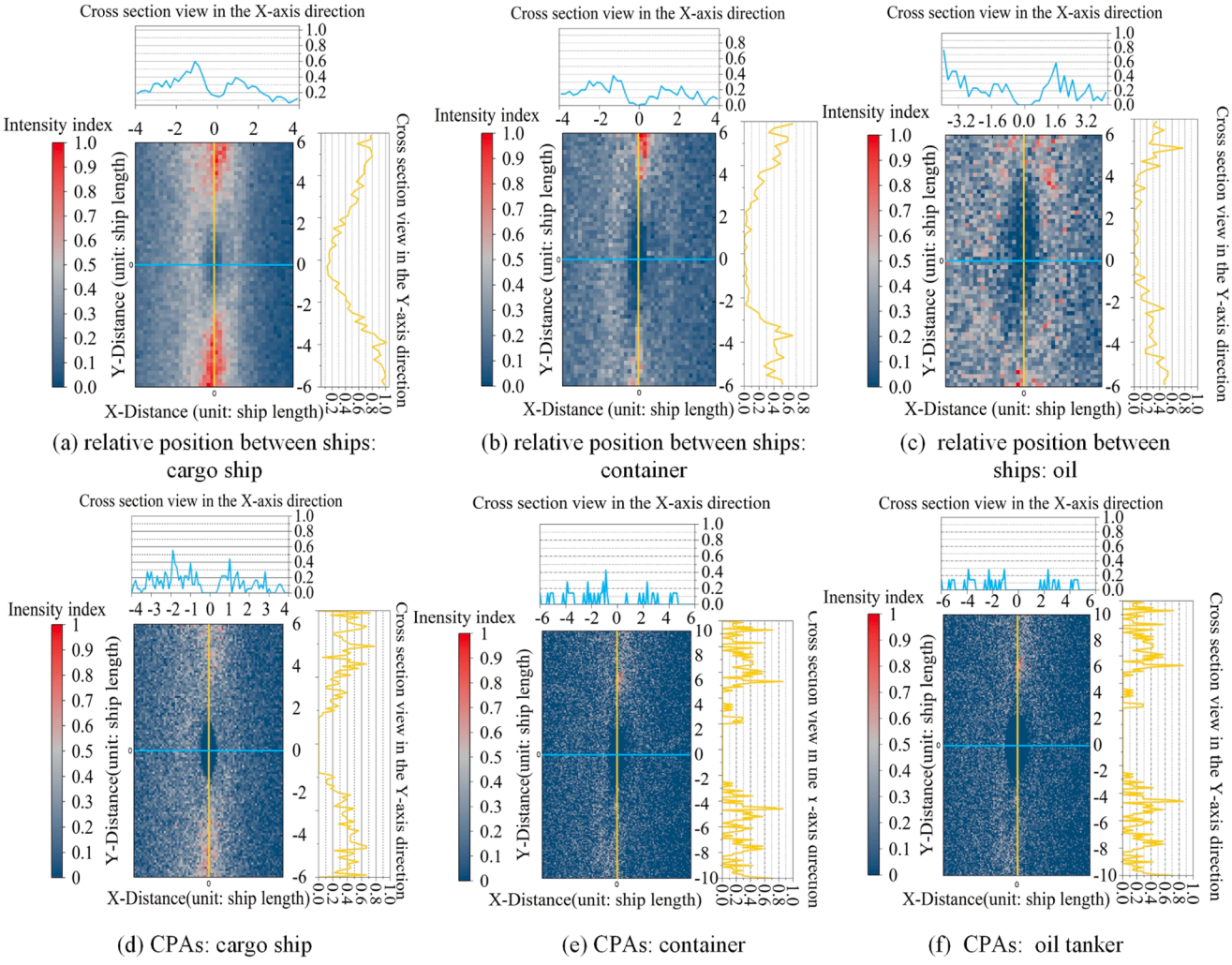

Fig. 11. Heatmap: relative position between ships & CPAs.

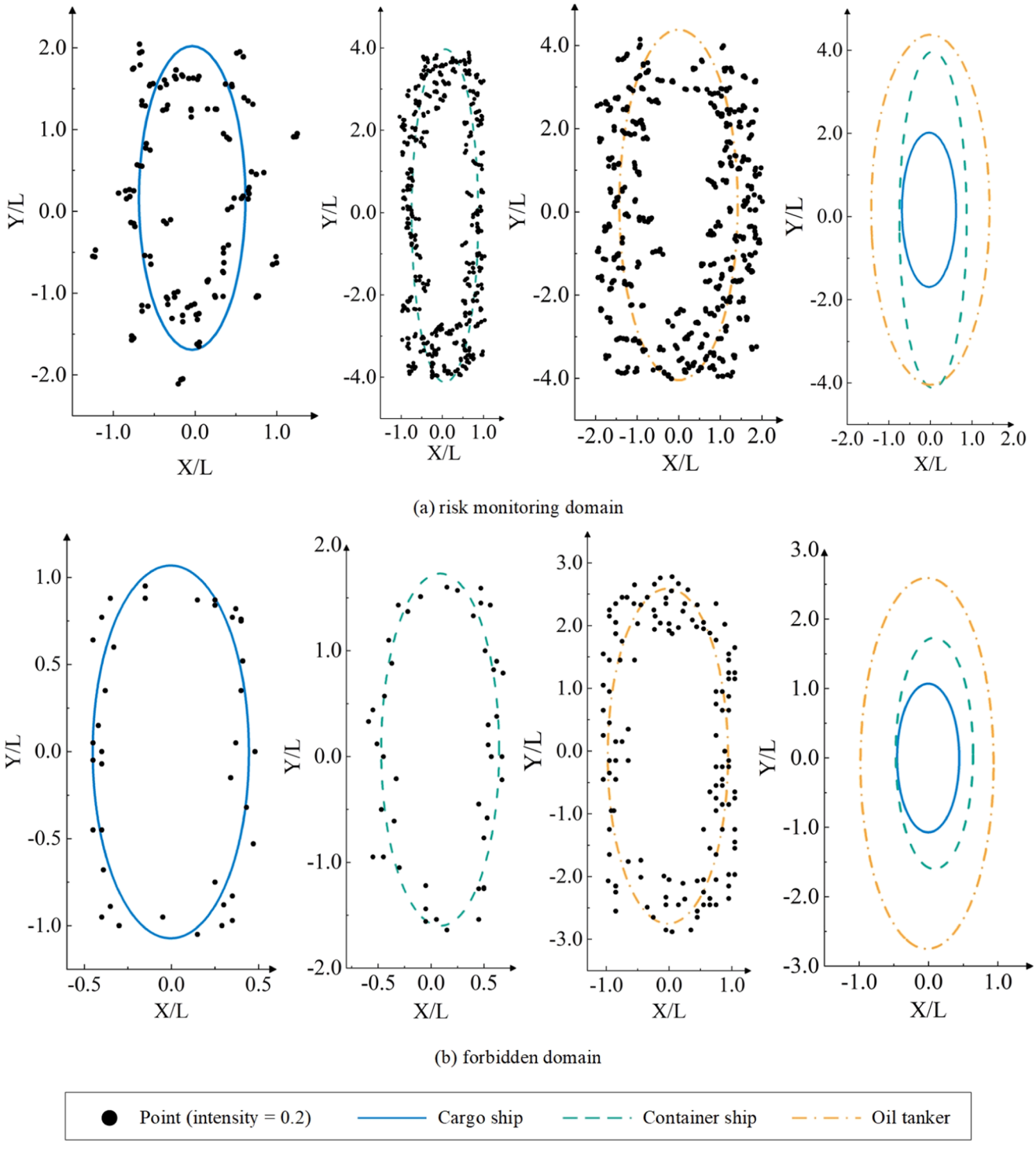

Fig. 12. Spatiotemporal risk monitoring domain.

Table 3
Parameter table of the risk monitoring domain model.

Ship type	$x_c(L)$	$y_c(L)$	$a(L)$	$b(L)$
Cargo ship	−0.03562	0.09361	0.61479	1.94903
Container ship	0.05043	−0.03185	0.82526	4.04729
Oil tanker	−0.00411	0.10305	1.42387	4.20973

Table 4
Parameter table of the forbidden domain model.

Ship type	$x_c(L)$	$y_c(L)$	$a(L)$	$b(L)$
Cargo ship	−0.00356	−0.03561	0.44825	1.11928
Container ship	0.08574	0.06479	0.55730	1.66490
Oil tanker	−0.02014	−0.08032	0.98560	2.67047

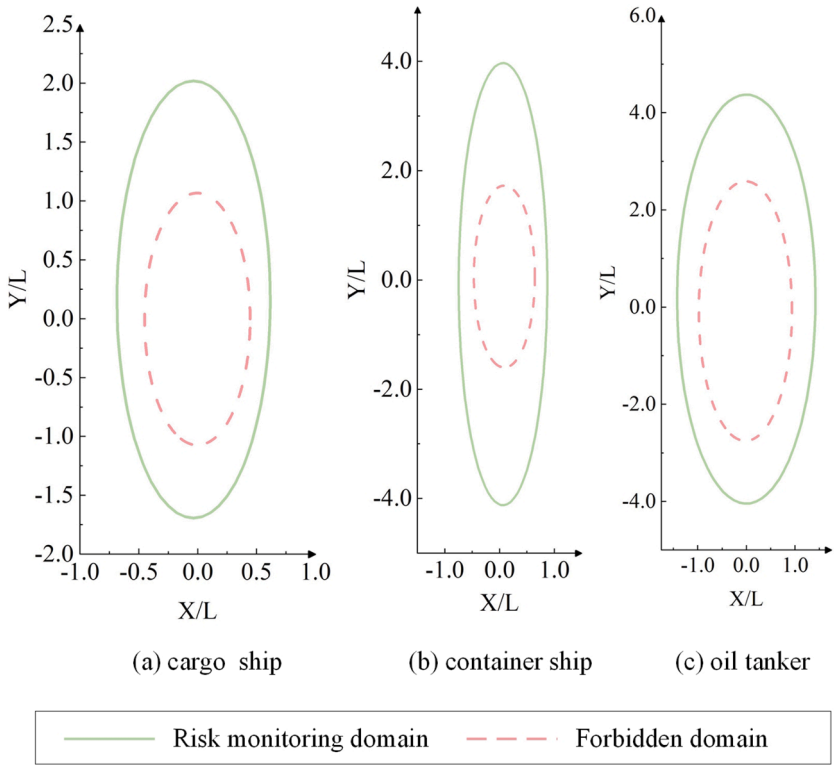

Fig. 13. Spatiotemporal risk monitoring domain: risk monitoring domain & forbidden domain.

Table 5
Ship information in crossing encounter scenarios.

Ship	MMSI	Type	Length (m)	Width (m)
A	412,436,260	Container ship	75.0	10.0
B	413,921,000	Cargo ship	162.0	26.0

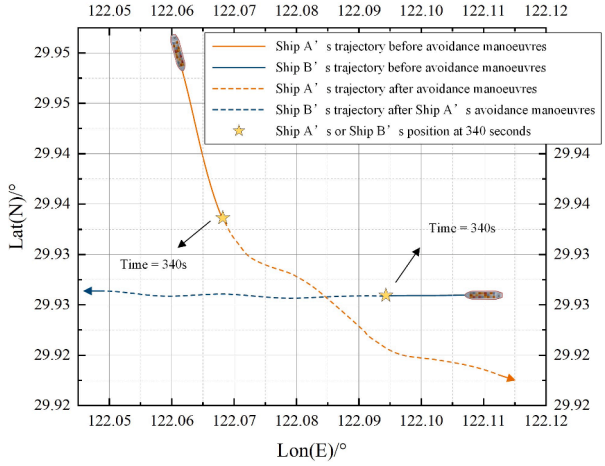

Fig. 14. Diagram of crossing encounter scenarios.

illustrated in Figs. 14 and 15.

The dynamic target risk analysis reveals several critical moments during the encounter. At 340 s, Ship A's risk value increased from 0 to 0.0101, coinciding with its collision avoidance manoeuvre. The risk peaked at 0.79381 at 637 s, corresponding to the minimum relative distance of 225.54 m and maximum relative and closing speeds. A significant risk reduction occurred at 646 s, dropping from 0.79286 to 0.50794, as the ships transitioned from approach to separation phase. The risk ultimately dissipated at 784 s, with the negative approaching speed indicating rapid separation between the ships. Fig. 16 illustrates the dynamic target risk variations throughout this crossing encounter.

An overtaking scenario involves two cargo ships (Ship C and Ship D), with their specifications detailed in Table 6. In accordance with the International Regulations for Preventing Collisions at Sea (COLREG) rules, Ship C assumes the give-way responsibility whilst Ship D maintains course as the stand-on ship. At 683 s into the encounter, Ship C executes a port turn manoeuvre, successfully passing on Ship D's port side. The encounter trajectories and parameter variations are illustrated in Fig. 17 and Fig. 18.

The overtaking scenario demonstrates distinct risk characteristics compared to crossing encounters, featuring prolonged close-proximity operations and gradual risk escalation prior to avoidance manoeuvres. The dynamic target risk value exhibited a steady increase from 0.3342 to 0.4742 before 683 s when Ship C initiated its port turn and acceleration for overtaking. At 997 s, Ship C, positioned on the port side of Ship D, executed a starboard turn, elevating the risk value to 0.5411. The overtaking completion at 1054 s resulted in a risk reduction to 0.4807, with both ships achieving initial stability. Subsequently, Ship D's speed increase diminished the relative distance, causing the risk value to peak at 0.6872 at 1448 s. Ship C's subsequent starboard turn increased separation, and at 1661 s, the negative closing speed confirmed mutual separation. The risk completely dissipated by 2395 s. Fig. 19 illustrates these dynamic target risk variations throughout the overtaking scenario.

4.3.2. Dynamic target risk in multi-ship encounter scenarios

A multi-ship encounter scenario involves three ships (Ships E, F, and G), with their detailed specifications presented in Table 7. The encounter comprises Ship E approaching from northwest to southeast, whilst Ships F and G proceed from east to west. At 300 s into the encounter, Ship E executes a port turn manoeuvre, enabling all three ships to maintain safe separation distances throughout the passage. The encounter trajectories and parameter variations are illustrated in

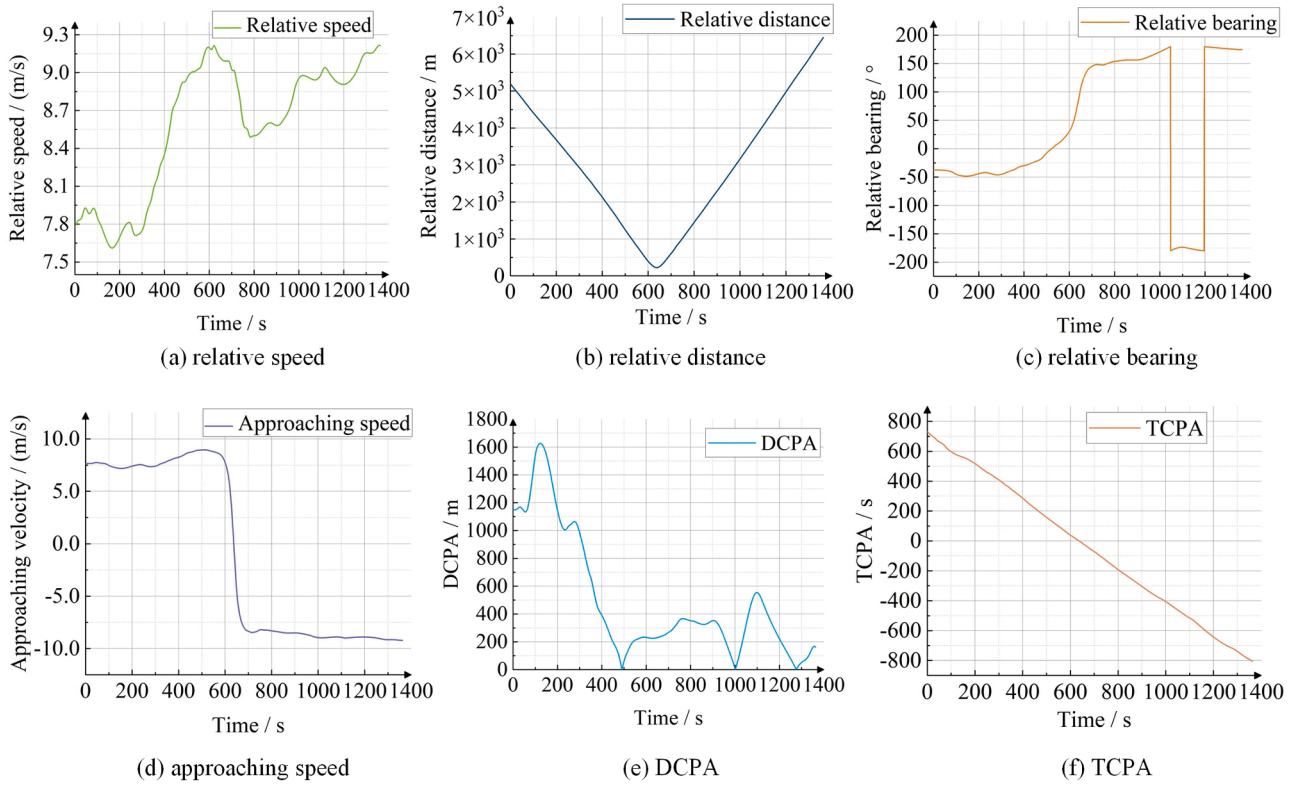

Fig. 15. Parameter diagram of crossing encounter scenarios.

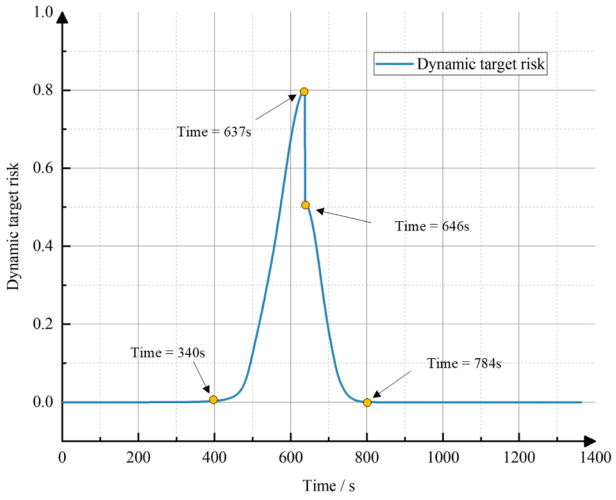

Fig. 16. Dynamic target risk of crossing encounter scenarios.

Table 6
Ship information in overtaking encounter scenarios.

Ship	MMSI	Type	Length (m)	Width (m)
C	412,433,130	Cargo ship	98.0	16.0
D	413,439,510	Cargo ship	60.0	14.0

Figs. 20 and 21.

The multi-ship encounter analysis reveals distinct risk patterns between Ship E and its interaction partners. The risk between Ships E and F initially exceeded 0.1 at 326 s, peaking at 0.5786 at 524 s. A significant risk reduction occurred at 556 s, dropping from 0.5474 to 0.2363, coinciding with the transition from positive to negative approach speed.

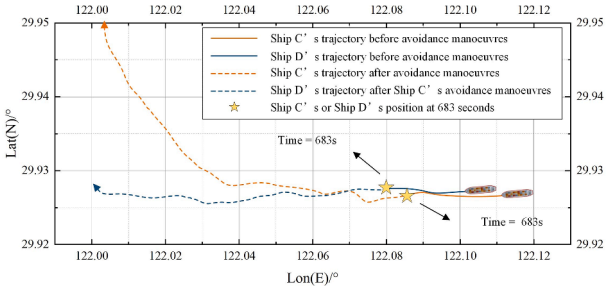

Fig. 17. Diagram of overtaking encounter scenarios.

This risk subsequently diminished below 0.1 by 623 s. The interaction between Ships E and G showed risk elevation beyond 0.1 at 426 s, reaching its maximum of 0.9500 at 702 s. A marked decrease from 0.9471 to 0.4829 occurred at 710 s, corresponding to the shift in approach speed direction. The risk subsided below 0.1 by 830 s. The fusion risk analysis demonstrated earlier sensitivity, exceeding 0.1 at 288 s. It exhibited two notable peaks: a secondary peak of 0.7050 at 555 s, followed by an immediate reduction to 0.5056 as Ships E and F separated, and a primary peak of 0.9504 at 702 s. The fusion risk diminished below 0.1 at 830 s, marking the end of the critical interaction phase. Fig. 22 illustrates these dynamic risk variations throughout the multi-ship encounter.

4.4. *Multi-source heterogeneous navigation risks case*

The comprehensive assessment of navigational risk necessitates the integration of both static environmental and dynamic target risk components. Analysis of crossing encounters and multi-ship scenarios enables examination of ship-environment interactions and inter-ship influences, quantified through their respective risk values. The integration of these components through a multi-source risk quantification

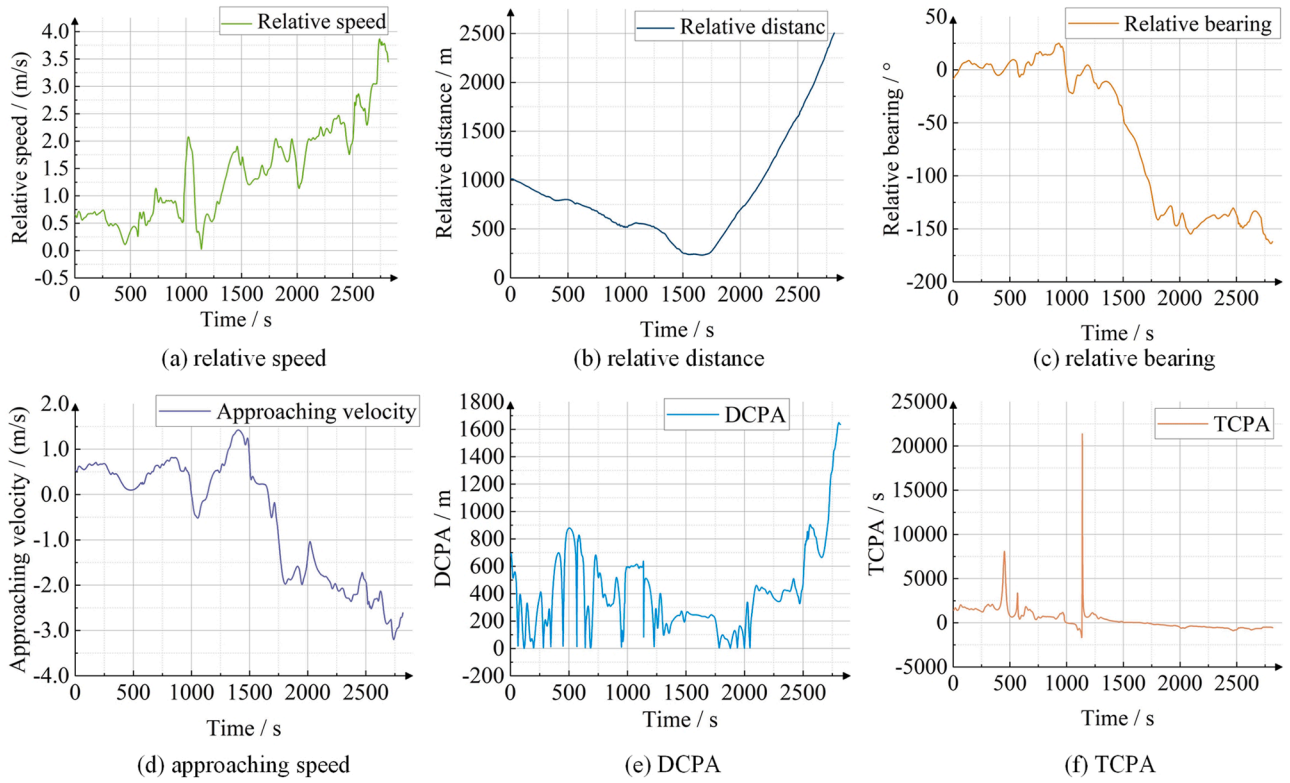

Fig. 18. Parameter diagram of overtaking encounter scenarios.

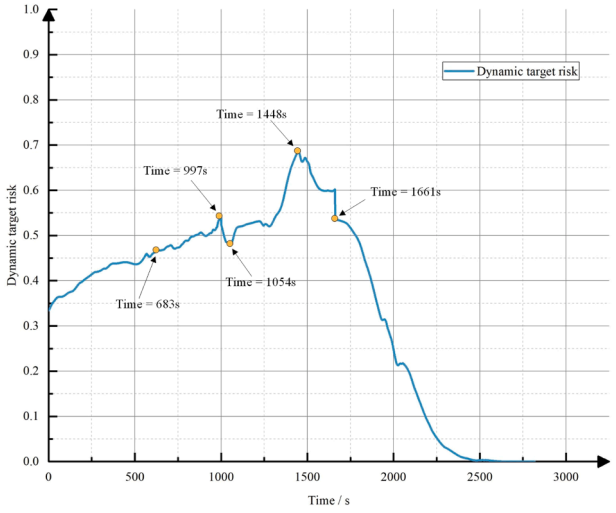

Fig. 19. Dynamic target risk of overtaking encounter scenarios.

Table 7
Ship information in multi-ship encounter scenarios.

Ship	MMSI	Type	Length (m)	Width (m)
E	416,077,000	Container	148.2	21.7
F	412,362,540	Cargo ship	72.0	12.0
G	413,275,680	Oil tanker	183.0	32.2

formula yields a total risk value, providing an accurate representation of overall navigational risk evolution. Having previously examined dynamic target risks in crossing and multi-ship encounters, subsequent analysis focuses on static environmental risk variations and their integration into total risk assessment.

4.4.1. Ship crossing encounter scenarios

The static environmental risk for Ship A manifests primarily across three temporal phases: initial navigation (0–87 s), channel entry (600–758 s), and pre-channel exit (1167–1363 s). During initial navigation, the risk value initiates at 0.3737 and diminishes rapidly, reflecting proximity hazards to an island and potential deviation into non-navigable areas. The risk subsides as Ship A progresses southeastward, increasing distance from the island.

The channel entry phase at 600 s marks peak static environmental risk, attributed to the ship's proximity to channel boundaries. This risk metric indicates potential channel deviation probability rather than definitive accident occurrence. The risk subsequently decreases as the ship establishes greater separation from channel boundaries. The pre-channel exit phase, commencing at 1167 s, exhibits renewed risk elevation due to proximity to channel margins.

The total risk assessment in crossing encounters amalgamates static environmental and dynamic target risks, with significant multi-source risk integration occurring between 340–784 s. The total risk profile predominantly mirrors static environmental risk patterns, with notable elevation at 340 s due to increasing dynamic target risk during the crossing encounter. A marked risk spike occurs at 600 s, driven by heightened static environmental risk, followed by a rapid decline as both risk components diminish. Fig. 23 illustrates these multi-source navigational risk variations throughout the crossing encounter.

4.4.2. Multi-ship encounter scenarios

Ship E's static environmental risk manifests across three distinct phases: initial navigation (0–67 s), channel entry (616–709 s), and channel exit (1160–1204 s). The initial phase commences with a risk value of 0.3869, diminishing rapidly thereafter. This elevated initial risk stems from proximity to an island, presenting potential drift hazards into non-navigable areas. The risk subsides as Ship E progresses southeastward, establishing greater separation from the island.

The channel entry phase at 616 s exhibits peak static environmental risk due to proximity to channel boundaries. Risk levels subsequently

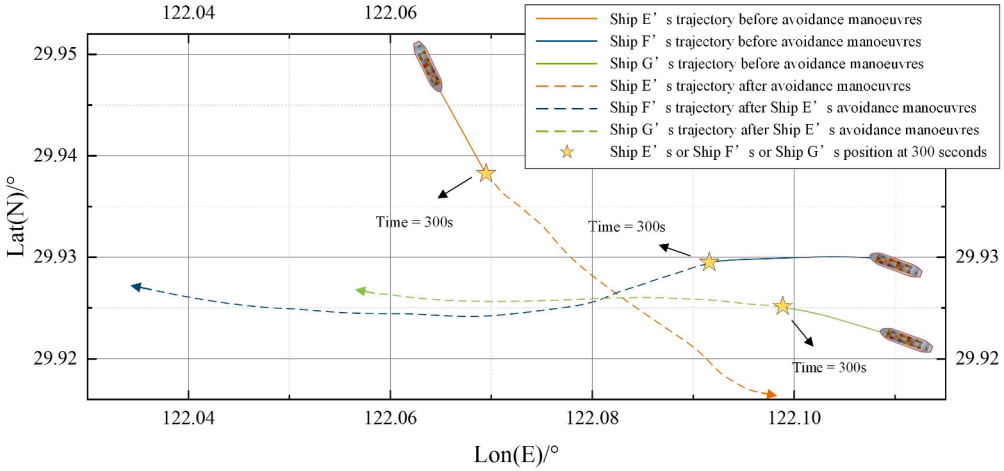

Fig. 20. Diagram of multi-ship encounter scenarios.

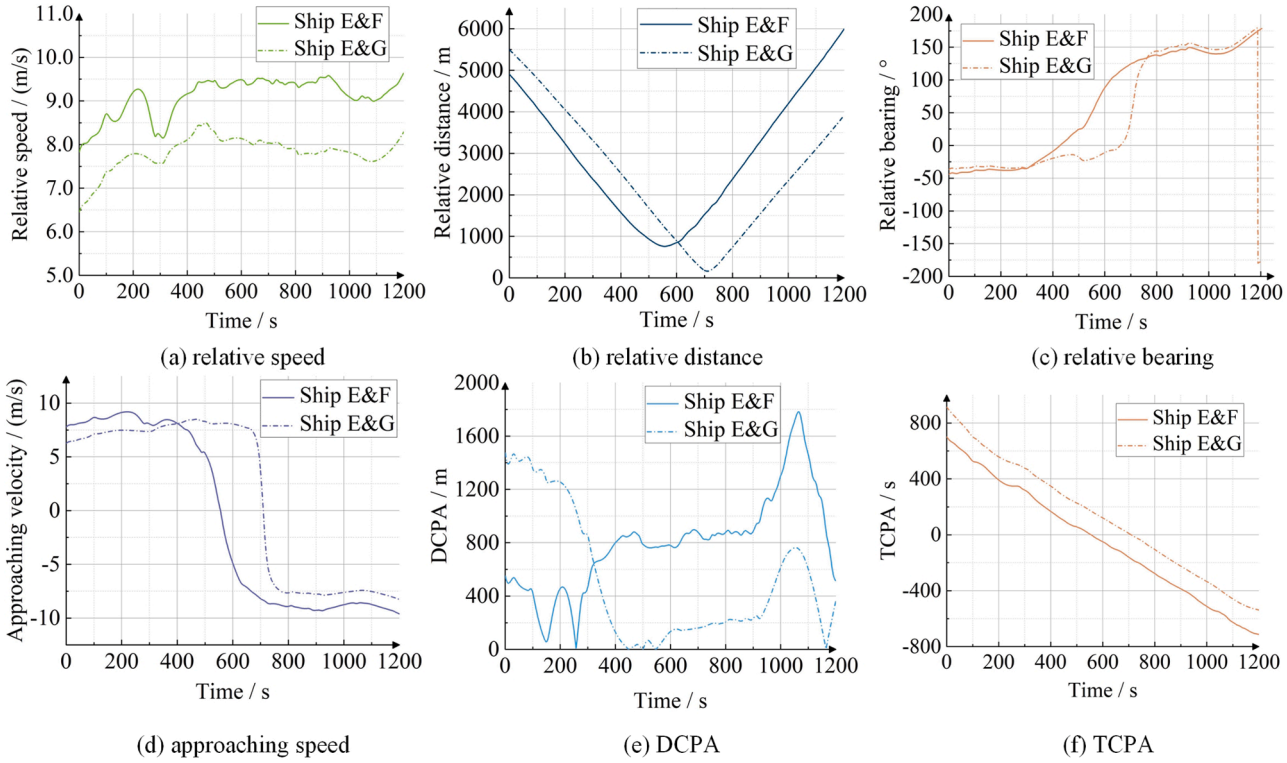

Fig. 21. Parameter diagram of multi-ship encounter scenarios.

decrease as the ship establishes greater separation from these boundaries. The channel exit phase, beginning at 1160 s, demonstrates renewed risk elevation due to reduced channel boundary margins.

The total risk assessment in the multi-ship encounter scenario integrates static environmental and dynamic target risks, with significant integration occurring between 288–830 s. The risk profile exhibits three distinct peaks. The first peak (0.7050) at 555 s, coinciding with the maximum Ship E-F dynamic target risk. The second peak (0.9955) at 627 s, reflecting the concurrent high static environmental risk and Ship E-G dynamic target risk. The third peak (0.9520) at 698 s, driven by peak Ship E-G dynamic target risk despite minimal static environmental risk. The risk profile initiates rapid elevation at 288 s due to concurrent risk acceleration between Ships E-F and E-G, subsequently declining following the final peak. Fig. 24 illustrates these multi-source navigational risk variations throughout the encounter.

5. Discussion and implications

5.1. discussion of the proposed framework

This study presents a quantitative fusion evaluation framework for assessing multi-source and heterogeneous navigation risks during ship voyages. The framework comprises four key components:

(1) Modelling spatio-temporal risk monitoring domains

A model integrating risk monitoring and forbidden areas for ships was developed through AIS data mining. This data-driven approach mitigates subjective biases, offering a clearer depiction of spatio-temporal ship distributions. Our model defines a more precise forbidden area, derived from the distribution of CPA data, thereby identifying critical areas for various dynamic and

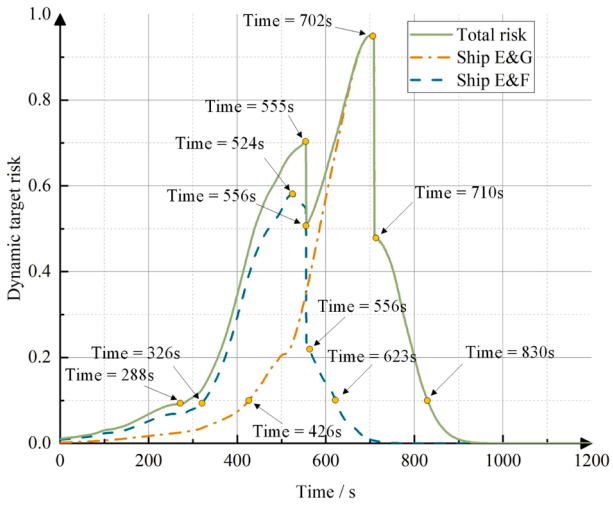

Fig. 22. Dynamic target risk of multi-ship encounter scenarios.

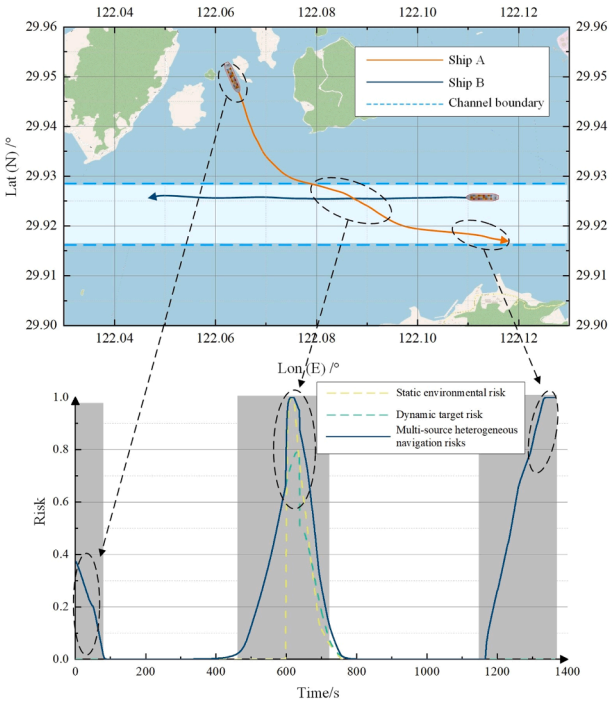

Fig. 23. Multi-source heterogeneous navigation risks of crossing encounter scenarios.

static obstacles. Unlike previous works, which relied on direct contact to determine risk, our forbidden area quantifies the threshold for potential accidents, significantly enhancing risk monitoring accuracy.

(2) Designing risk assessment functions

Heterogeneous navigation risks were categorised into dynamic target risks and static environmental risks, with asymmetric Gaussian-based assessment functions developed for each category. Risk levels are highest near the ship's centre and diminish with distance, modulated by four adaptive radius parameters that reflect ship size. This variation captures the differing sensitivities of ship officers to risks originating from various directions. Notably, the proposed model assigns a lower decay rate to dynamic target risks compared to static risks, effectively reflecting the heightened sensitivity to moving threats.

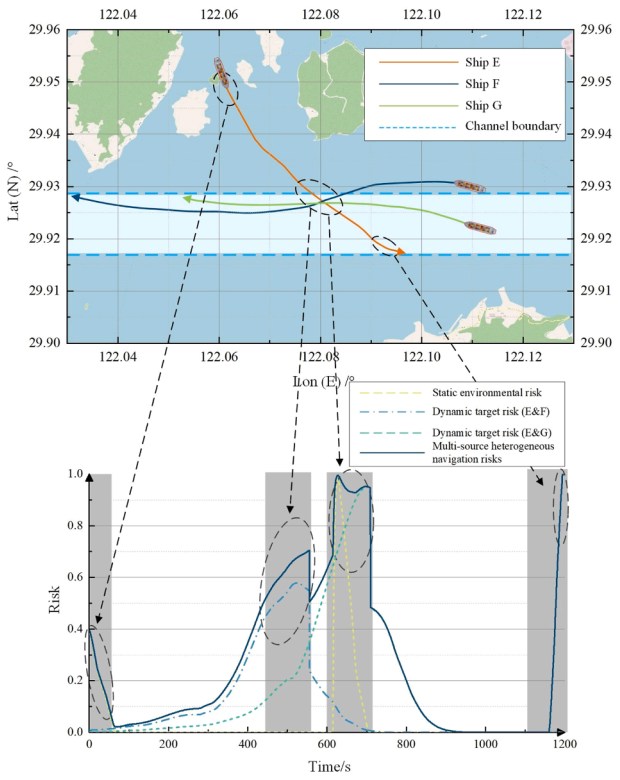

Fig. 24. Multi-source heterogeneous navigation risks of multi-ship encounter scenarios.

(3) Quantifying navigation risks

The proposed approach incorporates adaptive risk quantification methods tailored to different hazards. By assessing the overlap of spatio-temporal risk monitoring domains, dynamic target risks are characterised more effectively than through traditional methods, which often oversimplify interactions by considering ships and obstacles solely as point masses. Additionally, static environmental risks are assessed by examining their overlap with non-navigable areas. This method acknowledges the impact of ship size on risk levels and incorporates spatio-temporal dynamics, addressing limitations in prior studies.

(4) Fusing multi-source heterogeneous risks

The risk fusion model integrates diverse risk types—static environmental risks and dynamic target risks—while accounting for multiple sources in multi-ship scenarios. The model operates under three principles: 1) the maximum navigation risk is capped at 1, preventing cumulative risk values from exceeding this threshold; 2) the comprehensive risk value remains below 1 when no individual risk reaches this maximum; and 3) risk values are constrained to non-negative values. Distinct fusion functions for static and dynamic risks were developed, utilising a multiplicative equation to prevent inflated risk values. Additionally, a comprehensive fusion equation was designed to adapt to varying risk magnitudes. This multi-tiered approach ensures precise overall risk assessments while responding effectively to diverse navigation risks, thereby enhancing maritime safety evaluations.

This study exhibits certain limitations in the modelling of environmental and human factors. On one hand, the modelling of environmental factors primarily focuses on local features, such as waterway width and obstacle distribution, while the dynamic risks under complex environmental conditions (e.g., extreme weather and tidal variations) lack systematic analysis, potentially affecting the model's applicability and accuracy. On the other hand, the impact of human factors has not

been fully quantified, particularly the complexity of interactions between human operational behaviour and environmental conditions in emergency scenarios, which has not been effectively incorporated into the model. These limitations may constrain the comprehensiveness and practicality of the model in real-world maritime risk assessment.

5.2. Theoretical and practical of implications

Based on the discussion above, the implications of each point are as follows:

(1) Advancements in spatio-temporal risk monitoring.
This study presents a novel spatio-temporal risk monitoring model based on AIS data mining, offering improved maritime risk prediction. By employing a precise forbidden domain to define critical proximity thresholds, it surpasses traditional contact-based methods. This advancement enables more accurate risk assessment and timely decision-making, marking progress in data-driven maritime safety.
(2) Innovative risk evaluation functions.
The study introduces asymmetrical Gaussian-based risk functions to distinguish between dynamic and static risks, reflecting ship officers' directionally varying sensitivities. By prioritising dynamic obstacles, the tailored evaluation functions capture the heightened awareness needed for moving threats. This approach enhances traditional models with adaptive risk assessments closely aligned to real-world maritime operations.
(3) Refined navigation risk quantification.
The proposed risk quantification method goes beyond simple spatial measures by including both spatial and temporal dimensions. By evaluating the degree of overlap between ships' spatio-temporal monitoring fields, the model considers ship size and movement evolution, offering a dynamic risk measure that adapts to different ship encounter scenarios. This methodology addresses the limitations of previous studies, providing early warnings by evaluating the threat posed when obstacles enter the forbidden domain. It enhances early risk detection, providing actionable insights for proactive navigation risk management.
(4) Comprehensive multi-source risk fusion.
The study's multi-source risk fusion model effectively integrates various types of navigation risks, from static environmental risks to dynamic collision risks. By setting a cap on the maximum risk level and dynamically adjusting fusion coefficients, the model prevents risk overaccumulation while maintaining sensitivity to individual risk sources. This layered fusion approach enables an accurate, balanced risk assessment that can support safer maritime navigation, offering a reliable framework for managing diverse and complex risk scenarios. This methodology not only improves overall maritime safety but also sets a new standard for risk sensitivity in multi-source maritime risk assessments.

The implications for various stakeholders are summarised as follows:

The study's advancements in spatio-temporal risk monitoring and navigation risk quantification provide port authorities with improved tools for managing ship traffic, reducing collision risks, and optimising traffic flow. These frameworks enable proactive hazard mitigation, safer navigation, and more efficient resource allocation.

Regulators benefit from enhanced risk evaluation functions and multi-source risk fusion models, which offer a dynamic framework for setting safety standards and assessing compliance. This approach aligns with real-world conditions, enabling more precise guidelines for acceptable risk levels and supporting the development of modern regulatory frameworks.

For ship operators and crews, the study introduces adaptive risk functions that account for dynamic and static risks, offering real-time monitoring and early warnings. These features support safer navigation by improving awareness of immediate threats and enabling informed decision-making to reduce accidents.

The study also assists insurers by refining risk assessment processes through more comprehensive factors, including ship routes, port activities, and traffic density. This enables data-driven premium evaluations, improving risk management and incentivising safer operations across the industry.

Developers of maritime navigation technologies can leverage the study's models to create advanced tools integrating spatio-temporal risk monitoring and multi-source risk fusion. Such innovations are particularly valuable for autonomous ships, which rely on precise real-time data for safe navigation.

Lastly, accurate risk monitoring benefits environmental stakeholders by reducing the likelihood of collisions and groundings that could harm marine ecosystems. These insights support mitigation planning and promote the protection of sensitive environments in high-risk areas.

By addressing these diverse needs, the study fosters a cohesive maritime safety ecosystem, enhancing operational efficiency, navigational safety, and environmental protection across the sector.

6. Conclusions

This paper presents a novel framework for the quantification and integration of multi-source heterogeneous navigation risks in maritime environments. The framework addresses the challenges associated with fusing and quantifying the diverse risks encountered by ships during navigation. Real ship trajectory data from typical scenarios, including crossing encounters, overtaking, and multi-ship meetings, were utilised to analyse navigation risks.

This paper distinguishes itself from previous research in several key aspects. First, a spatiotemporal risk monitoring domain model was developed by mining historical AIS data. Through analysis of the relative positional distribution of ships and patterns of CPAs, risk monitoring and forbidden domains were extracted, enabling the quantification of risk monitoring timings. Second, heterogeneous navigation risk evaluation functions were designed using asymmetric Gaussian functions to capture ships' sensitivity to different types and directions of risks. Finally, an adaptive-weighted risk fusion method, grounded in mariner risk perception, was proposed to enable the integrated representation of multi-source heterogeneous navigation risks.

Future work will prioritise improving the model's accuracy by integrating dynamic environmental factors, including wind, waves, currents, and tides, to better capture environmental variability. Furthermore, incorporating human factors into risk quantification, such as leveraging maritime accident data to assess the influence of human errors on evaluation outcomes, will enhance the model's comprehensiveness and reliability.

CRediT authorship contribution statement

Lichao Yang: Writing – original draft, Visualization, Validation, Methodology. **Jingxian Liu:** Supervision, Funding acquisition. **Qin Zhou:** Writing – review & editing, Supervision. **Zhao Liu:** Supervision, Methodology. **Yang Chen:** Data curation. **Yukuan Wang:** Visualization. **Yang Liu:** Validation.

Declaration of competing interest

The authors declare that they have no known competing financial interests or personal relationships that could have appeared to influence the work reported in this paper.

Acknowledgements

This study was supported by the National Natural Science

Foundation of China (Grant Nos. 52471383, 52171351) and the Qingdao Key Technology Research project (Grant No. 24-1-3-hygg-8-hy). The first author has been supported by the scholarship from the China Scholarship Council (CSC) under Grant No. 202406950117, and he also acknowledges helpful support and guidance from Dr Huanhuan Li at Liverpool John Moores University.

Data availability

The data that has been used is confidential.

References

[1] Liang M, Li H, Liu RW, Lam JSL, Yang Z. PiracyAnalyzer: spatial temporal patterns analysis of global piracy incidents. Reliab Eng Syst Saf 2024;243:109877. https://doi.org/10.1016/j.ress.2023.109877.
[2] Liu P, Xu Y, Xie X, Turkmen S, Fan S, Ghassemi H, et al. Achieving the global net-zero maritime shipping goal: the urgencies, challenges, regulatory measures and strategic solutions. Ocean Coast Manage 2024;256:107301. https://doi.org/10.1016/j.ocecoaman.2024.107301.
[3] Wang Y, Liu J, Liu RW, Liu Y, Yuan Z. Data-driven methods for detection of abnormal ship behavior: progress and trends. Ocean Eng 2023;271:113673. https://doi.org/10.1016/j.oceaneng.2023.113673.
[4] Liang M, Weng L, Gao R, Li Y, Du L. Unsupervised maritime anomaly detection for intelligent situational awareness using AIS data. Knowl Based Syst 2024;284:111313. https://doi.org/10.1016/j.knosys.2023.111313.
[5] Jovanović I, Perčić M, BahooToroody A, Fan A, Vladimir N. Review of research progress of autonomous and unmanned shipping and identification of future research directions. J Mar Eng Technol 2024;23:82–97. https://doi.org/10.1080/20464177.2024.2302249.
[6] Li H, Xing W, Jiao H, Yang Z, Li Y. Deep bi-directional information-empowered ship trajectory prediction for maritime autonomous surface ships. Transp Res Part E: Logist Transp Rev 2024;181:103367. https://doi.org/10.1016/j.tre.2023.103367.
[7] Liu Y, Liu J, Zhang Q, Liu Y, Wang Y. Effect of dynamic safety distance of heterogeneous traffic flows on ship traffic efficiency: a prediction and simulation approach. Ocean Eng 2024;294:116660. https://doi.org/10.1016/j.oceaneng.2023.116660.
[8] Chin HC, Debnath AK. Modeling perceived collision risk in port water navigation. Saf Sci 2009;47:1410–6. https://doi.org/10.1016/j.ssci.2009.04.004.
[9] Chen P, Huang Y, Mou J, van Gelder PHAJM. Probabilistic risk analysis for ship-ship collision: state-of-the-art. Saf Sci 2019;117:108–22. https://doi.org/10.1016/j.ssci.2019.04.014.
[10] Liu Z, Zhang B, Zhang M, Wang H, Fu X. A quantitative method for the analysis of ship collision risk using AIS data. Ocean Eng 2023;272:113906. https://doi.org/10.1016/j.oceaneng.2023.113906.
[11] Chen Y, Liu Z, Zhang M, Yu H, Fu X, Xiao Z. Dynamics collision risk evaluation and early alert in busy waters: a spatial-temporal coupling approach. Ocean Eng 2024;300:117315. https://doi.org/10.1016/j.oceaneng.2024.117315.
[12] Lee H-J, Furukawa Y, Park D-J. Seafarers' awareness-based domain modelling in restricted areas. J Navig 2021;74:1172–88. https://doi.org/10.1017/S0373463321000394.
[13] Szlapczynski R, Szlapczynska J. Review of ship safety domains: models and applications. Ocean Eng 2017;145:277–89. https://doi.org/10.1016/j.oceaneng.2017.09.020.
[14] Wielgosz M, Pietrzykowski Z. The ship domain in navigational safety assessment. PloS One 2022;17:e0265681. https://doi.org/10.1371/journal.pone.0265681.
[15] Silveira P, Teixeira AP, Guedes SC. A method to extract the quaternion ship domain parameters from AIS data. Ocean Eng 2022;257:111568. https://doi.org/10.1016/j.oceaneng.2022.111568.
[16] Galić S, Lušić Z, Mladenović S, Gudelj A. A chronological overview of scientific research on ship grounding frequency estimation models. J Mar Sci Eng 2022;10:207. https://doi.org/10.3390/jmse10020207.
[17] Deeb H, Mehdi RA, Hahn A. A review of damage assessment models in the maritime domain. Ships Offshore Struc 2017;12:S31–54. https://doi.org/10.1080/17445302.2016.1278317.
[18] Zhang WZ, Pan J, Sanchez JC, Li XB, Xu MC. Review on the protective technologies of bridge against vessel collision. Thin-Walled Struct 2024;201:112013. https://doi.org/10.1016/j.tws.2024.112013.
[19] Rawson A, Brito M. Assessing the validity of navigation risk assessments: a study of offshore wind farms in the UK. Ocean Coast Manage 2022;219:106078. https://doi.org/10.1016/j.ocecoaman.2022.106078.
[20] Son W-J, Cho I-S. Optimal maritime traffic width for passing offshore wind farms based on ship collision probability. Ocean Eng 2024;313:119498. https://doi.org/10.1016/j.oceaneng.2024.119498.
[21] Xue H, Chai T. Bimodal distribution–based collision probability of ship with buoy in two-way navigable channel. ASCE-ASME J Risk Uncertain Eng Systems, Part A: Civ Eng 2024;10:04024010. https://doi.org/10.1061/AJRUA6.RUENG-1149.
[22] Zhou Y, Li X, Yuen KF. Holistic risk assessment of container shipping service based on Bayesian network modelling. Reliab Eng Syst Saf 2022;220:108305. https://doi.org/10.1016/j.ress.2021.108305.
[23] Fan C, Montewka J, Bolbot V, Zhang Y, Qiu Y, Hu S. Towards an analysis framework for operational risk coupling mode: a case from MASS navigating in restricted waters. Reliab Eng Syst Saf 2024;248:110176. https://doi.org/10.1016/j.ress.2024.110176.
[24] Zhang X, Chen W, Xi Y, Hu S, Tang L. Dynamics simulation of the risk coupling effect between maritime pilotage human factors under the HFACS framework. J Mar Sci Eng 2020;8:144. https://doi.org/10.3390/jmse8020144.
[25] Wan C, Zhao Y, Zhang D, Fan L. A system dynamics-based approach for risk analysis of waterway transportation in a mixed traffic environment. Marit Policy Manag 2024;51:1147–69. https://doi.org/10.1080/03088839.2023.2224328.
[26] Li H, Çelik C, Bashir M, Zou L, Yang Z. Incorporation of a global perspective into data-driven analysis of maritime collision accident risk. Reliab Eng Syst Saf 2024;249:110187. https://doi.org/10.1016/j.ress.2024.110187.
[27] Xin X, Liu K, Loughney S, Wang J, Yang Z. Maritime traffic clustering to capture high-risk multi-ship encounters in complex waters. Reliab Eng Syst Saf 2023;230:108936. https://doi.org/10.1016/j.ress.2022.108936.
[28] Liu J, Zhang J, Yang Z, Wan C, Zhang M. A novel data-driven method of ship collision risk evolution evaluation during real encounter situations. Reliab Eng Syst Saf 2024;249:110228. https://doi.org/10.1016/j.ress.2024.110228.
[29] Zhang M, Kujala P, Hirdaris S. A machine learning method for the evaluation of ship grounding risk in real operational conditions. Reliab Eng Syst Saf 2022;226:108697. https://doi.org/10.1016/j.ress.2022.108697.
[30] Fu S, Yu Y, Chen J, Xi Y, Zhang M. A framework for quantitative analysis of the causation of grounding accidents in arctic shipping. Reliab Eng Syst Saf 2022;226:108706. https://doi.org/10.1016/j.ress.2022.108706.
[31] Dinis D, Teixeira AP, Guedes SC. Probabilistic approach for characterising the static risk of ships using Bayesian networks. Reliab Eng Syst Saf 2020;203:107073. https://doi.org/10.1016/j.ress.2020.107073.
[32] Li H, Yang Z. Towards safe navigation environment: the imminent role of spatio-temporal pattern mining in maritime piracy incidents analysis. Reliab Eng Syst Saf 2023;238:109422. https://doi.org/10.1016/j.ress.2023.109422.
[33] Deng J, Liu S, Xie C, Liu K. Risk coupling characteristics of maritime accidents in Chinese inland and coastal waters based on N-K model. J Mar Sci Eng 2022;10:4. https://doi.org/10.3390/jmse10010004.
[34] Zhao Y, Li W, Shi P. A real-time collision avoidance learning system for unmanned surface vessels. Neurocomputing 2016;182:255–66. https://doi.org/10.1016/j.neucom.2015.12.028.
[35] Bukhari AC, Tusseyeva I, lee B-G, Kim Y-G. An intelligent real-time multi-vessel collision risk assessment system from VTS view point based on fuzzy inference system. Expert Syst Appl 2013;40:1220–30. https://doi.org/10.1016/j.eswa.2012.08.016.
[36] Ahn J-H, Rhee K-P, You Y-J. A study on the collision avoidance of a ship using neural networks and fuzzy logic. Appl Ocean Res 2012;37:162–73. https://doi.org/10.1016/j.apor.2012.05.008.
[37] Li B, Pang F-W. An approach of vessel collision risk assessment based on the D–S evidence theory. Ocean Eng 2013;74:16–21. https://doi.org/10.1016/j.oceaneng.2013.09.016.
[38] Goerlandt F, Montewka J, Kuzmin V, Kujala P. A risk-informed ship collision alert system: framework and application. Saf Sci 2015;77:182–204. https://doi.org/10.1016/j.ssci.2015.03.015.
[39] Liu Z, Wu Z, Zheng Z. A cooperative game approach for assessing the collision risk in multi-vessel encountering. Ocean Eng 2019;187:106175. https://doi.org/10.1016/j.oceaneng.2019.106175.
[40] Ma W, Zhu Y, Grifoll M, Liu G, Zheng P. Evaluation of the effectiveness of active and passive safety measures in preventing ship–bridge collision. Sens 2022;22:2857. https://doi.org/10.3390/s22082857.
[41] Fujii Y, Shiobara R. The analysis of traffic accidents. J Navig 1971;24:534–43. https://doi.org/10.1017/S0373463300022372.
[42] Altan YC. Collision diameter for maritime accidents considering the drifting of vessels. Ocean Eng 2019;187:106158. https://doi.org/10.1016/j.oceaneng.2019.106158.
[43] Yang L, Liu J, Liu Z, Luo W. Grounding risk quantification in channel using the empirical ship domain. Ocean Eng 2023;286:115672. https://doi.org/10.1016/j.oceaneng.2023.115672.
[44] Pedersen P. Collision and grounding mechanics. The Danish Society of Naval Architects and Marine Engineers; 1995. p. 125–57.
[45] Youssef SAM, Paik JK. Hazard identification and scenario selection of ship grounding accidents. Ocean Eng 2018;153:242–55. https://doi.org/10.1016/j.oceaneng.2018.01.110.
[46] Khaled M.E., Kawamura Y., Abdullah M.S.B., Banik A., Faruk A.K., Khan M.R. Assessment of collision & grounding risk at Chittagong Port, Bangladesh, 2018.
[47] Sakar C, Toz AC, Buber M, Koseoglu B. Risk analysis of grounding accidents by mapping a fault tree into a bayesian network. Appl Ocean Res 2021;113:102764. https://doi.org/10.1016/j.apor.2021.102764.
[48] Jiang D, Wu B, Cheng Z, Xue J, van Gelder PHAJM. Towards a probabilistic model for estimation of grounding accidents in fluctuating backwater zone of the three gorges reservoir. Reliab Eng Syst Saf 2021;205:107239. https://doi.org/10.1016/j.ress.2020.107239.
[49] Abaei MM, Arzaghi E, Abbassi R, Garaniya V, Javanmardi M, Chai S. Dynamic reliability assessment of ship grounding using Bayesian inference. Ocean Eng 2018;159:47–55. https://doi.org/10.1016/j.oceaneng.2018.03.039.
[50] Liu L, Zhang M, Hu Y, Zhu W, Xu S, Yu Q. A probabilistic analytics method to identify striking ship of ship-buoy contact at coastal waters. Ocean Eng 2022;266:113102. https://doi.org/10.1016/j.oceaneng.2022.113102.

[51] Wu B, Yip TL, Yan X, Guedes Soares C. Fuzzy logic based approach for ship-bridge collision alert system. Ocean Eng 2019;187:106152. https://doi.org/10.1016/j.oceaneng.2019.106152.
[52] Yu Q, Liu K, Chang C-H, Yang Z. Realising advanced risk assessment of vessel traffic flows near offshore wind farms. Reliab Eng Syst Saf 2020;203:107086. https://doi.org/10.1016/j.ress.2020.107086.
[53] Bakdi A, Glad IK, Vanem E. Testbed scenario design exploiting traffic big data for autonomous ship trials under multiple conflicts with collision/grounding risks and spatio-temporal dependencies. IEEE Trans Intell Transp Syst 2021;22:7914–30. https://doi.org/10.1109/TITS.2021.3095547.
[54] Lyu H, Yue J, Zhang W, Cheng T, Yin Y, Yang X, et al. Fatigue detection for ship OOWs based on input data features, from the perspective of comparison with vehicle drivers: a review. IEEE Sensors J 2023;23:15239–52. https://doi.org/10.1109/JSEN.2023.3281068.
[55] Liang M, Su J, Liu RW, Lam JSL. AISClean: AIS data-driven vessel trajectory reconstruction under uncertain conditions. Ocean Eng 2024;306:117987. https://doi.org/10.1016/j.oceaneng.2024.117987.